ORNL/TM-2015/225

Final Report:

Evaluation of Variable Refrigerant Flow Systems Performance and the Enhanced Control Algorithm on Oak Ridge National Laboratory's Flexible Research Platform

Piljae Im, PhD
Jeffrey D. Munk
Anthony C. Gehl

June 3, 2015

OAK RIDGE NATIONAL LABORATORY
MANAGED BY UT-BATTELLE FOR THE US DEPARTMENT OF ENERGY

Energy and Transportation Science Division

Final Report:

Evaluation of Variable Refrigerant Flow Systems Performance and the Enhanced Control Algorithm on Oak Ridge National Laboratory's Flexible Research Platform

Piljae Im, PhD
Jeffrey D. Munk
Anthony C. Gehl

Date Published: June 3, 2015

Prepared by
OAK RIDGE NATIONAL LABORATORY
Oak Ridge, Tennessee 37831-6283
managed by
UT-BATTELLE, LLC
for the
US DEPARTMENT OF ENERGY
under contract DE-AC05-00OR22725

EXECUTIVE SUMMARY

A research project *"*Evaluation of Variable Refrigerant Flow (VRF) Systems Performance and the Enhanced Control Algorithm on Oak Ridge National Laboratory's (ORNL's) Flexible Research Platform*"* was performed to (1) install and validate the performance of Samsung VRF systems compared with the baseline rooftop unit (RTU) variable-air-volume (VAV) system and (2) evaluate the enhanced control algorithm for the VRF system on the two-story flexible research platform (FRP) in Oak Ridge, Tennessee.

Based on the VRF system designed by Samsung and ORNL, the system was installed from February 18 through April 15, 2014. The final commissioning and system optimization were completed on June 2, 2014, and the initial test for system operation was started the following day, June 3, 2014. In addition, the enhanced control algorithm was implemented and updated on June 18. After a series of additional commissioning actions, the energy performance data from the RTU and the VRF system were monitored from July 7, 2014, through February 28, 2015. Data monitoring and analysis were performed for the cooling season and heating season separately, and the calibrated simulation model was developed and used to estimate the energy performance of the RTU and VRF systems.

This final report includes discussion of the design and installation of the VRF system, the data monitoring and analysis plan, the cooling season and heating season data analysis, and the building energy modeling study.

1. Design and installation of the VRF system

The two-story FRP is a small office building with ten thermal zones (i.e., eight perimeter zones and two core zones), and the selected VRF system comprises one outdoor condensing unit and ten indoor units (six wall-mounted and four ceiling units). The total cooling and heating capacities of the condensing unit are about 144 and 162 MBH, respectively, and the ten indoor units' cooling and heating capacities range from 7.5 to 18 MBH and from 8.5 to 20 MBH, respectively. The rated energy efficiency ratio (EER) and integrated EER for the outdoor condensing unit are 11.2 and 22.7, respectively.

In addition to a conventional thermostatic control system for the VRF system, an enhanced control algorithm (CCM) was implemented. The initial algorithm with the Zensys system was implemented on April 28 through May 2, 2014, and the initial CCM algorithm was updated remotely by Samsung on June 18, 2014. The updated control will automatically switch the VRF system with set point and CCM control with the planned schedule.

2. Data monitoring and analysis plan

The FRP is instrumented with temperature and relative humidity sensors in each room, as well as a variety of sensors to measure the weather. In addition to the existing sensors, more sensors were installed to measure overall energy use and delivered heating or cooling in each zone. To compare different

heating, ventilation, and air-conditioning (HVAC) systems and controls, three different scenarios were performed every week by switching the system or controls. The three scenarios are (1) baseline RTU with thermostatic control, (2) VRF system with thermostatic control only, and (3) VRF with CCM control.

The performance of the VRF system was analyzed by comparing the weather normalized energy use for each system/control and comparing the indoor thermal conditions. Two different metrics were used for the evaluation. First, the hourly indoor temperature for each thermal zone for the different systems was compared with the thermostat set point to see if the system could provide adequate cooling and heating for the zones. Second, predicted mean vote (PMV) values were calculated to evaluate the thermal comfort of the zones.

3. Cooling Season Data Analysis

Cooling season data were monitored from July 7 through September 30, 2014. The zone set point temperature was set to 24°C during occupied hours (i.e., 6 a.m. to 6 p.m.), and the setback temperature, 30°C, was set for unoccupied hours. The data were analyzed by plotting the hourly energy consumption of each system during occupied hours against the corresponding hourly average outdoor air (OA) temperature. The data show little or no difference in energy consumption for the RTU and the VRF in higher OA temperature ranges (e.g., over 30°C) and show that the VRF system used less energy in lower OA temperature ranges. This finding was expected because of the better part-load performance of VRF systems compared with the RTU. In addition, data show increased energy use for the RTU system below 15°C because of the VAV reheat energy use. Using the weather-normalized models for the RTU, VRF–thermostat, and VRF–CCM systems, the energy savings during the cooling season were estimated. The analysis shows that the VRF system with thermostatic control and CCM control would save about 17 and 26% of HVAC energy use, respectively, compared with the RTU. When CCM control is compared with conventional control for the VRF, CCM control would save about 10% of the HVAC energy use.

The cooling season indoor thermal comfort analysis shows that the VRF system with thermostatic control can provide a similar or better level of thermal comfort compared with the RTU system. The median zone temperature for RTU operation shows that the zones are slightly overcooled (1 to 2°C), particularly the rooms downstairs. During VRF CCM operation, several rooms showed close to 30°C maximum zone temperatures, which are likely to be uncomfortable for most occupants. Further algorithm updates would be considered to improve thermal comfort for the zones, especially for the perimeter zones.

4. Heating Season Data Analysis

Heating season data were monitored from October 1, 2014, through February 28, 2015. The zone set point temperature was set to 21°C during occupied hours, and the setback temperature, 15.5 °C, was set for unoccupied hours. The data were analyzed by plotting the daily energy consumption of each system against the corresponding daily average OA temperature. The heating season data were analyzed using daily HVAC energy consumption data; the daily data serve better than the hourly data for the analysis because the heating season data show some HVAC energy consumption during unoccupied hours even with the setback temperature.

Based on the weather-normalized models developed for the RTU, VRF–thermostat, and VRF–CCM scenarios, daily energy use from October 1, 2014 through February 28, 2015 was estimated. The measured daily average OA temperature and the daily total global solar radiation for this period were used as independent variables. The modeled energy uses for RTU, VRF–thermostat, and VRF–CCM operation show that the VRF system with thermostatic control would use 74% less energy than the RTU system; and the VRF system with CCM control would use 80% less energy than the RTU system. Comparing VRF–thermostat and VRF–CCM control, it seems CCM control would use around 23% less energy than thermostatic control.

The heating season indoor thermal comfort analysis shows the VRF system with thermostatic control can provide a similar level of thermal comfort to the RTU system. The median zone temperature for RTU operation shows that the zones are a bit underheated, particularly the rooms downstairs. It appears that several perimeter zones would require cooling while other zones still require heating. Since the current heat pump–type VRF system cannot provide simultaneous cooling and heating, there is a potential risk for uncomfortable thermal conditions. A heat recovery–type of VRF system is likely to resolve that issue, though. The median zone temperatures for VRF–CCM control show a similar pattern to VRF–thermostatic control but with more variations, which is expected because of a larger dead band.

5. Energy Modeling Analysis

In addition to the field measurement data, an hourly building energy model was used to analyze the energy performance of the RTU and VRF systems and to compare the annual energy consumption for the two systems. The initial building energy models for the RTU and VRF systems were developed using EnergyPlus 8.1 and calibrated using the daily energy use for both systems. The calibrated model, simulated with the 2014 actual weather data for Oak Ridge, Tennessee, estimated that the VRF system would use about 60% less energy (i.e., 31,649 kWh/year less) than the RTU system. This figure included 71% (21,415 kWh/year) heating energy savings, 22% (2,787 kWh/year) cooling energy savings, and 78% (i.e., 7,448 kWh/year) fan energy savings.

When an OA reset schedule was applied to the RTU discharge air temperature in the calibrated model, the RTU cooling and heating energy use decreased by about 706 kWh (6%) and 5,280kWh (18%), respectively. As a result, it is estimated that the VRF will use 55% less HVAC energy than the RTU system.

When both an OA reset schedule and hot water reheating with 80% natural gas boiler were applied to the RTU calibrated model, the VRF system would use 33% less HVAC-related source energy compared with the RTU system.

CONTENTS

LIST OF FIGURES

LIST OF TABLES

Page

1. INTRODUCTION

1.1 Background

Multi-split air-conditioning systems, or variable refrigerant flow (VRF) systems, are relatively new in the US market, although they have been used in many countries in Europe and Asia for more than 25 years. The known benefits of VRF systems include (1) easier modular installation (particularly beneficial for building retrofits), (2) space savings due to having one outdoor unit connected to multiple indoor units, (3) ability to respond to fluctuations in space load conditions, (4) easier and more cost-effective maintenance and commissioning, and (5) energy efficiency. However, several studies show that there are concerns regarding the application of VRF systems in the United States, including (1) lack of awareness of the energy-efficiency advantages, (2) higher initial cost, and (3) code compliance issues specific to the United States. These concerns need to be resolved to expedite the market penetration of VRF systems in the United States.

To address the concerns regarding VRF systems, there have been numerous studies of multi-split VRF systems since they were introduced in Japan about 30 years ago. Most studies were performed as field and chamber experiments and/or energy modeling analyses to verify the energy efficiency of VRF systems. In general, field experiments were performed with a set of VRF indoor units and an outdoor unit, and their energy consumption and performance were analyzed in real buildings under several different scenarios (e.g., by varying the indoor loads, control modes, and ventilation). The field studies verified the measured cooling/heating performance of the VRF systems under those various conditions, although it was relatively hard to compare VRF performance with that of other heating, ventilation, and air-conditioning (HVAC) systems in the same building. Energy modeling studies have often been used to compare VRF system performance with the performance of other HVAC systems in a building under the same conditions. Sometimes modeling studies use generic building models to compare the performance and energy consumption of VRF and other HVAC systems, or use a calibrated model for the same analysis. Although calibrated simulation would provide better analysis results, it is still limited in predicting the precise energy consumption of the alternative systems in real buildings because of uncertainties in the model algorithm itself and with regard to occupant behavior and the operational schedules of the building.

An ideal comparison between two systems can be performed only if energy use during the test period is free from the influence of occupancy and weather-related parameters, a situation hard to achieve in real buildings. Recently, Oak Ridge National Laboratory (ORNL) constructed two light commercial building flexible research platforms (FRPs) on the ORNL main campus: a single-story FRP and a two-story FRP. The two-story FRP exposes the “test buildings” to natural weather conditions for purposes of research and development (R&D) leading to system-/building-level advanced energy efficiency solutions for new and retrofit applications. A fixed building occupancy is emulated with preprogrammed portable heaters and humidifiers so that the variations in energy use among different systems are attributable only to system performance and weather. Variations in weather conditions can be normalized using air temperature normalization or calibrated simulation modeling.

1.2 Purpose/Objective

This research project aimed to install and validate the performance of VRF systems using the two-story FRP at ORNL. In addition, a newly developed integrated control system (i.e., the comfort control method [CCM]) for VRF systems was implemented to investigate the potential for additional energy savings and enhanced thermal comfort. For this project, two main research objectives are defined as follows:

1. To design and install the VRF system and monitoring systems on the two-story FRP, and monitor and evaluate the energy use and thermal comfort performance of the VRF system with conventional thermostatic control.
2. To implement the CCM with the VRF system, and monitor and evaluate the energy use and thermal comfort performance of the VRF system with CCM control vs. with conventional thermostatic control.

1.3 Organization of the Report

Chapter 2 includes a description of the ORNL's FRP, including the existing baseline HVAC system. Chapter 3 describes the design and installation of the VRF system in the two-story FRP and implementation of the enhanced control system (called "Zensys"). Chapter 4 describes the monitoring and analysis plan, including the instrumentation for the building and the systems. Chapters 5 and 6 present the cooling and heating season data analysis, respectively, to evaluate the energy use and thermal comfort performance of different HVAC operation scenarios. Chapter 7 discusses the annual energy analysis using a calibrated energy simulation. Finally, Chapter 8 concludes the study with a summary, findings, lessons, and discussion of future work.

2. FLEXIBLE RESEARCH PLATFORM

2.1 Introduction of FRPs

The FRPs at ORNL are a part of a multiyear project with the goal of installing temporary, instrumented baseline "test buildings" on two permanent FRPs (consisting of slabs and steel, Fig. 1). They were established as part of the American Recovery and Reinvestment Act–funded Maximum Energy Efficiency Laboratory (MAXLAB). The single-story FRP with a footprint of 40×60 ft (12×18 m) (Fig. 1b) and the two-story FRP with a footprint of 40×40 ft (12×12 m) (Fig. 1c) are able to physically simulate light commercial buildings common in the nation's existing building stock. The FRPs are an unoccupied research apparatus in which occupancy can be simulated by process control of lighting and other internal loads to minimize human interference with the building, which is one of the main sources of uncertainty in building energy use. These test buildings are exposed to the natural weather for purposes of research and development (R&D) leading to system-/building-level advanced energy efficiency solutions for new and retrofit applications. On these test buildings, tune-ups, retrofits, or alternative building components or systems can be implemented; and the data gathered with and without the modifications can be used to characterize the baseline energy performance and the energy savings from the tune-up/retrofit or alternative system/component. In addition, a dedicated weather station (Fig. 2) is installed on the roof of the two-story FRP so that the actual weather data can be used in performance analysis and energy modeling. For this project, the two-story FRP was used.

2.2 FRP with Baseline System

As a first step of the study, a baseline test building was defined based on a literature review (e.g., Commercial Buildings Energy Consumption Survey, the US Department of Energy's Benchmark model, and a previous version of American Society of Heating, Refrigerating and Air-Conditioning Engineers [ASHRAE] Standard 90.1(ASHRAE 1989) and communication with industry partner to be representative of a typical low-rise office building built in the United States in the 1990s. The building has ten conditioned zones, including two core zones and eight perimeter zones.

To simulate occupancy, sensible and latent heat additions are estimated and simulated using portable heaters and humidifiers with preprogrammed timers. The sensible heat from occupants and from other building equipment such as computers, copiers, and other office machinery is simulated with portable heaters and timers. The lighting fixtures are turned on and off based on the preprogrammed operational schedule.

The baseline systems in the FRP consist of a 12.5 ton rooftop unit (RTU) and a natural gas furnace. The RTU has a 9.6 energy efficiency rating (EER). The furnace has an 81% annual fuel utilization efficiency (AFUE) rating. Each room in the FRP has a variable air volume (VAV) box with electric resistance reheat. The central fan in the air-handling unit (AHU) draws return air from each room. Fresh air is introduced through the unit to provide adequate ventilation in accordance with ASHRAE standard 62.1-2013 (ASHRAE 2013). An exhaust fan is located on each floor and operates when the supply fan is running. The RTU is programmed to maintain a constant discharge air temperature at 14°C. The natural

gas furnace engages if the building mixed-air temperature drops below 14°C. As long as the discharge air is at least 14°C, the zone electric heat in the VAV boxes activates to provide the necessary perimeter heat. The baseline envelope and HVAC characteristics of the two-story test building are shown in Table 1.

Fig. 1. (a) FRP permanent apparatus, (b) single-story FRP, and (c) two-story FRP.

Fig. 2. Weather station on two-story FRP.

Table 1. Characteristics of the test building

General characteristics	
Location	Oak Ridge, Tennessee
Building width	40 ft (12.2 m)
Building length	40 ft (12.2 m)
Story height (floor to floor)	14 ft (4.3 m)
Number of floors	2
Number of thermal zones	10 (8 perimeter and 2 core zones)
Construction characteristics	
Wall structure	Concrete masonry units with face brick
Wall insulation	Fiberglas R_{US}-11 (R_{SI}-1.9)
Floor	Slab-on-grade
Roof structure	Metal deck with polyisocyanurate and ethylene proplylene diene monomer
Roof insulation	Polyisocyanurate R_{US} –18(R_{SI} –3.17)
Windows	Double-pane clear glazing
Window-to-wall ratio	28%
Systems and equipment characteristics	
Lighting power density	0.85 W/ft^2 (9.18W/m^2)
Equipment power density	1.3 W/ ft^2 (14.04W/m^2)
Baseline systems	Roof top unit with electric reheat, natural gas furnace
RTU cooling capacity	12.5 ton
RTU efficiency	9.7 EER
Natural gas furnace efficiency	81% AFUE

The performance of the system is evaluated using the refrigerant and air-side measurements. The room temperature and relative humidity (RH) and the supply, return, and mixed-air temperature and RH are monitored at 30 second intervals. For the HVAC system, compressor and fan power are measured individually and each individual room's reheat power is monitored. The baseline system performance is monitored using multiple sensors in the building:

- 35 temperature/RH probes (rooms, supply air duct, return and mixed air, VAV box, exhaust air, and outdoor air [OA])
- 6 refrigerant side immersion thermistors
- 6 refrigerant side pressure transducers
- 2 refrigerant mass flow sensors
- 1 natural gas mass flow meter
- 2 airflow measurement stations
- 16 HVAC power measurements
- 21 building end-use power measurements

3. DESIGN AND INSTALLATION OF VRF SYSTEM

3.1 FRP with VRF System

The sizing of the VRF system was determined from the load calculations using *Manual N* (Rutkowski 2008), and the corresponding indoor and outdoor units were chosen based on consultation with Samsung. Table 2 shows the specifications of the selected indoor/outdoor units. Fig. 3 shows the locations of the indoor units in different rooms on the first and second floors of the FRP. Figures 4 through 6 show pictures of the outdoor unit, a wall-mounted indoor unit, and a ceiling-mounted indoor unit, respectively. The outdoor condensing unit is equipped with two scroll compressors and is charged with R-410a. The total cooling and heating capacities of the condensing unit are about 144 MBH and 162 MBH, respectively. The cooling and heating capacities of the ten indoor units range from 7.5 to 18 MBH and from 8.5 to 20 MBH, respectively. The outdoor condensing unit has a rated performance of 11.2 EER and 22.7 IEER (integrated EER). Based on communication with Samsung, it was decided to compare the performance of different types of VRF indoor units; the final selected set of indoor units consisted of six wall-mounted systems and four ceiling-mounted 4-way systems. System installation began on February 18, 2014, and was completed on April 15, 2014, with the first commissioning performed by Samsung. The second and third commissioning were performed by Samsung on May 8 and 29, respectively, and the final commissioning and system optimization were performed by Samsung on June 2, 2014.

The VRF system design document from the VRF installer, included in Appendix A, shows the piping layout, wiring, and specifications of the indoor and outdoor units.

Table 2. Specification of VRF system indoor/outdoor units

Location		Name	Model name	Cooling capacity (Btu/h)	Sensible cooling capacity (Btu/h)	Heating capacity (Btu/h)
Ground (outside)		New outdoor	AM144FXVAFH/AA	144,000	-	162,000
Second floor	Rm 202	AC-21	AM012FNTDCH/AA	12,000	8,000	13,500
	Rm 203	AC-22	AM007FNTDCH/AA	7,500	5,100	8,500
	Rm 204	AC-23	AM018FNTDCH/AA	18,000	12,200	20,000
	Rm 205	AC-24	AM018FNNDCH/AA	18,000	13,600	20,000
	Rm 206	AC-25	AM018FNNDCH/AA	18,000	13,600	20,000
First floor	Rm 102	AC-11	AM007FNTDCH/AA	7,500	5,100	8,500
	Rm 103	AC-12	AM007FNTDCH/AA	7,500	5,100	8,500
	Rm 104	AC-13	AM018FNTDCH/AA	18,000	12,200	20,000
	Rm 105	AC-14	AM018FNNDCH/AA	18,000	13,600	20,000
	Rm 106	AC-15	AM018FNNDCH/AA	18,000	13,600	20,000

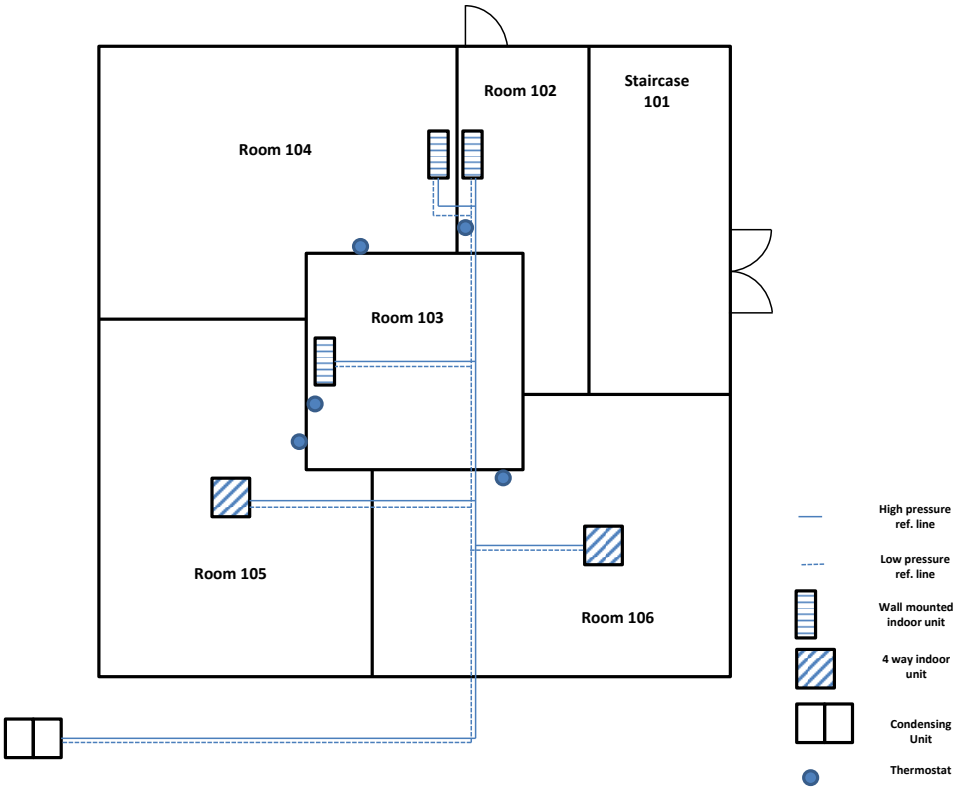

First Floor

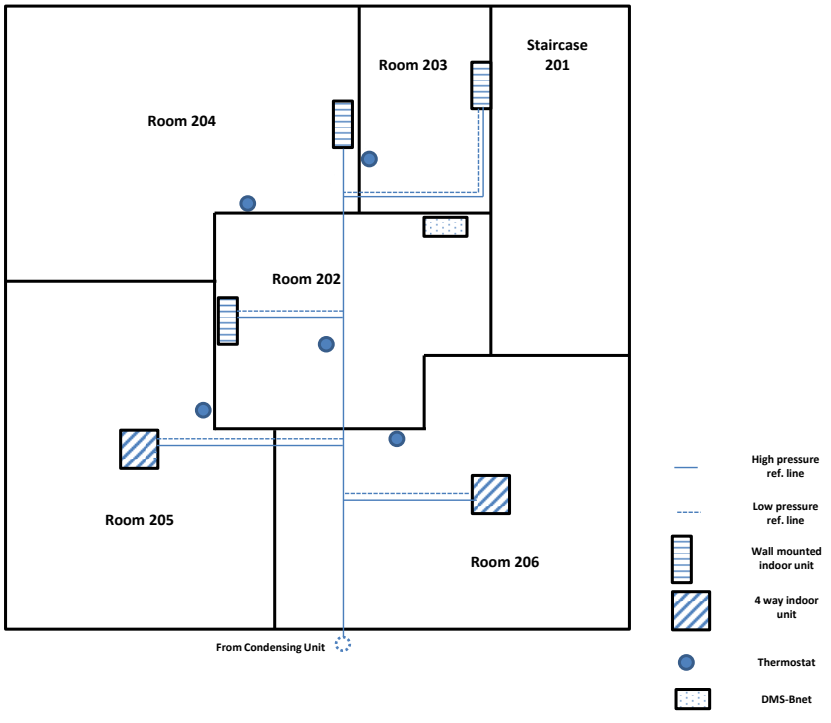

Second Floor

Fig. 3. Layout of the VRF systems on the first and the second floors of the FRP.

Fig. 4. Outdoor condensing unit.

Fig. 5. Wall-mounted indoor unit with thermostat.

Fig. 6. Ceiling-mounted indoor unit.

3.2 Implementation of CCM Algorithm

The enhanced control algorithm (CCM) was implemented from April 28 to May 2, 2014, after the VRF system was installed. The Zensys system, which is used to implement the CCM algorithm, was delivered to ORNL by Samsung, and the system was installed by ORNL under Samsung's direction. Figures 7 and 8 show the concept diagram of the FRP Zensys system and the actual installation of the Zensys system in the FRP, respectively. The system installation included

1. Installation of thermostat/RH sensor for each room (Fig. 9)
2. Wire connection from the sensors to the direct digital controller (DDC)
3. Installation and connection of DDC, master controller, and the dedicated PC

The software implantation was performed on-site by Samsung and included

1. Installation of the Zensys program
2. Installation of the binding sensor, DDC, MC, and PC
3. Implementation of the CCM algorithm
4. Partial test (system on/off test using the Zensys program)

The initial CCM algorithm was updated remotely by Samsung on June 18, 2014. The updated control would switch the VRF system with set point and with the CCM control automatically with the planned

schedule[1]. To perform further updates required for the Zensys, Samsung could connect to the PC remotely.

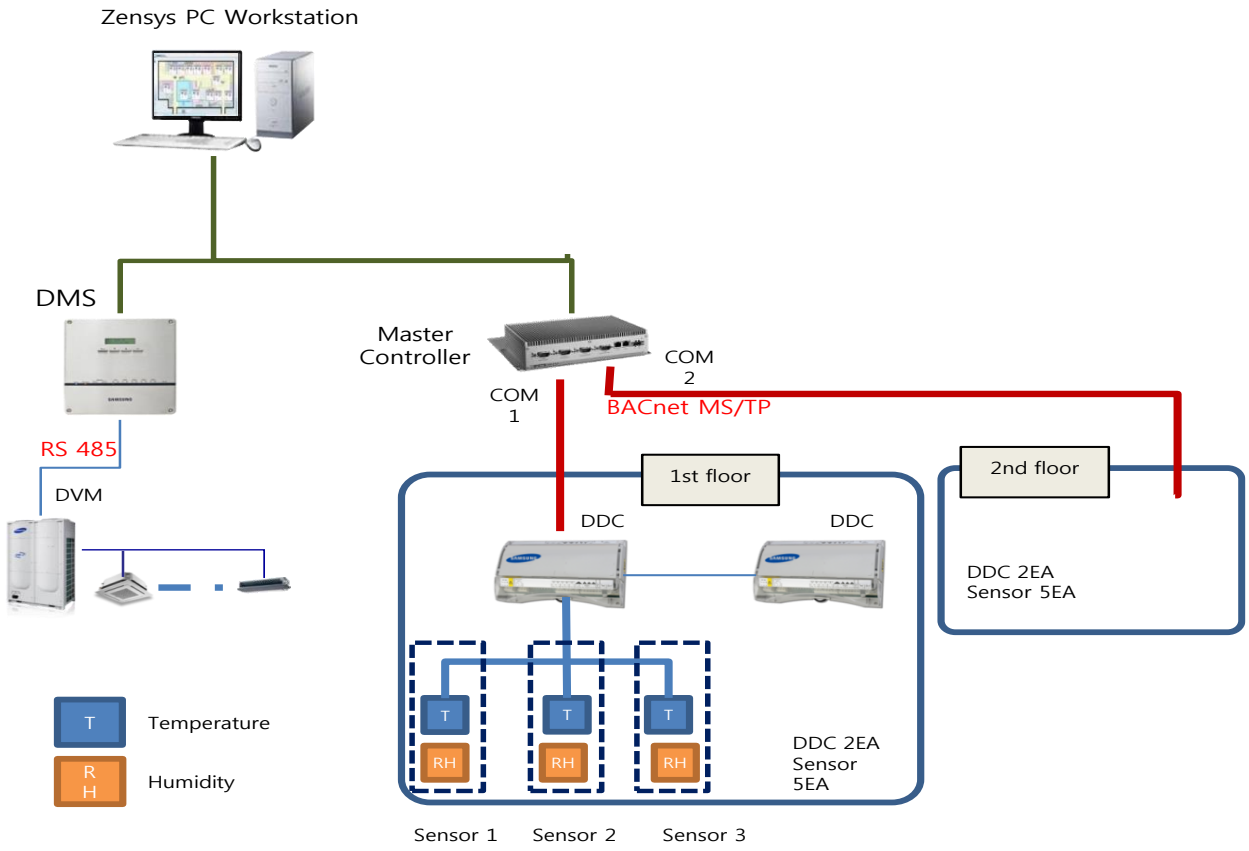

Fig. 7. Concept diagram for Zensys system in the two-story FRP.

[1]For the HVAC operational schedule, see Table 5.

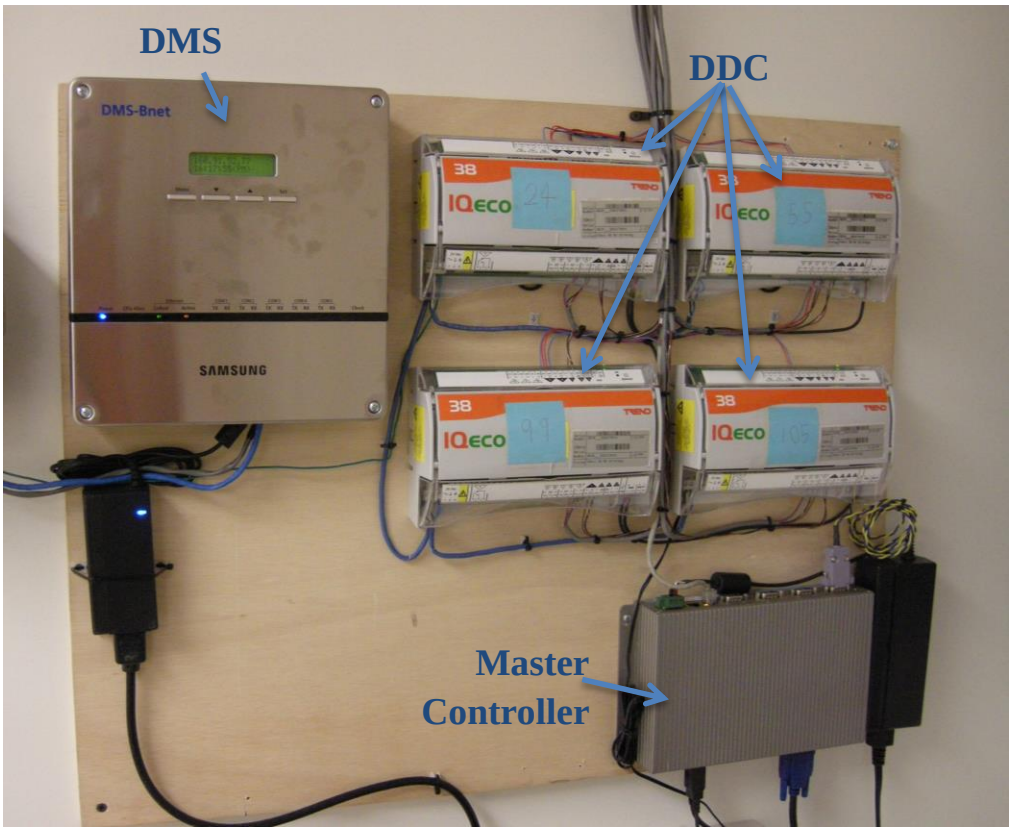

Fig. 8. Zensys system in the two-story FRP.

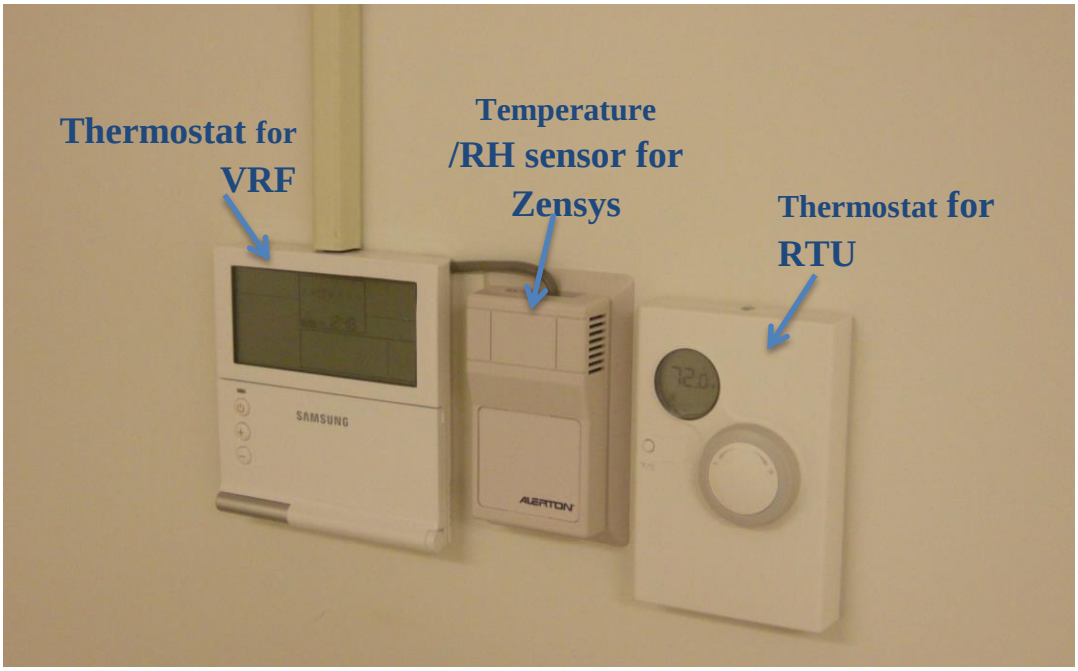

Fig. 9. Thermostat and temp/RH sensor.

4. MONITORING AND ANALYSIS PLAN

4.1 Data Measurement

The FRP is instrumented with temperature and RH sensors in each room and a variety of sensors to measure the weather. All the sensors are connected to a data acquisition system (DAS). The DAS for the two-story building consists of two Campbell Scientific model CR3000 data loggers used for acquiring and recording field data (Fig. 10). Each data logger is equipped with a number of input modules to accommodate various types of sensor inputs. One logger system is designed to measure the performance of the building envelope through temperature, humidity, heat flux, and differential pressures of the outside walls, windows, and roof. This system also includes a roof-mounted weather station. The second data logger system is designed to measure the performance of the building equipment, including the HVAC systems, as well as all of the building's electrical loads and the temperature and humidity of each room. All new sensors added to the DAS for monitoring the Samsung VRF system performance were connected to the second logger. Data are collected from both data loggers every 30 seconds and, for ease of use, are also averaged or totalized, as applicable, in 1 minute, 15 minute, 60 minute, and 24 hour tables.

The VRF system is instrumented for the overall energy use and delivered heating or cooling in each zone. The energy of the outdoor unit, as well as of the individual indoor units, is measured. Air-side measurements on each indoor unit can be used to measure the delivered capacity. The air-side measurements consist of return air and supply air temperature and RH measurements (Figs. 11 and 12). The fan speed of the indoor blowers is measured via an optical sensor and thin strip of reflective tape (Fig. 13). The fan speed and the power measurements of each indoor unit are correlated with the supply air volume (cubic feet per minute, CFM) based on the CFM specification from the manufacturer. Details for the VRF instrumentation are found in Table 3.

Table 3. List of VRF sensors

Function	Sensor	Sensor model	Location	Quantity	Accuracy
Cooling/ heating capacity	Temp/RH	Campbell Sci HC2S3-L	All air side	20	±0.1°C and ±0.1% RH @ 23°C
	RPM sensor	Reflective object sensors	All air side	10	N/A
Power	Wattnode	Continental Controls WNB-3D-240P, 100 hz option	ID units	11	±0.5% of reading
	CT	Continental Controls ACT-0750-005	ID units	22	±0.75% of reading
	Wattnode	Continental Controls WNB-3D-240P, 100 hz option	OD unit	1	±0.5% of reading
	CT	Continental Controls ACT-0750-020	OD unit	3	±0.75% of reading
Condensate	Rain gauge	Campbell Sci TB4MM-L	Condensate drain tube	1	±2% of reading

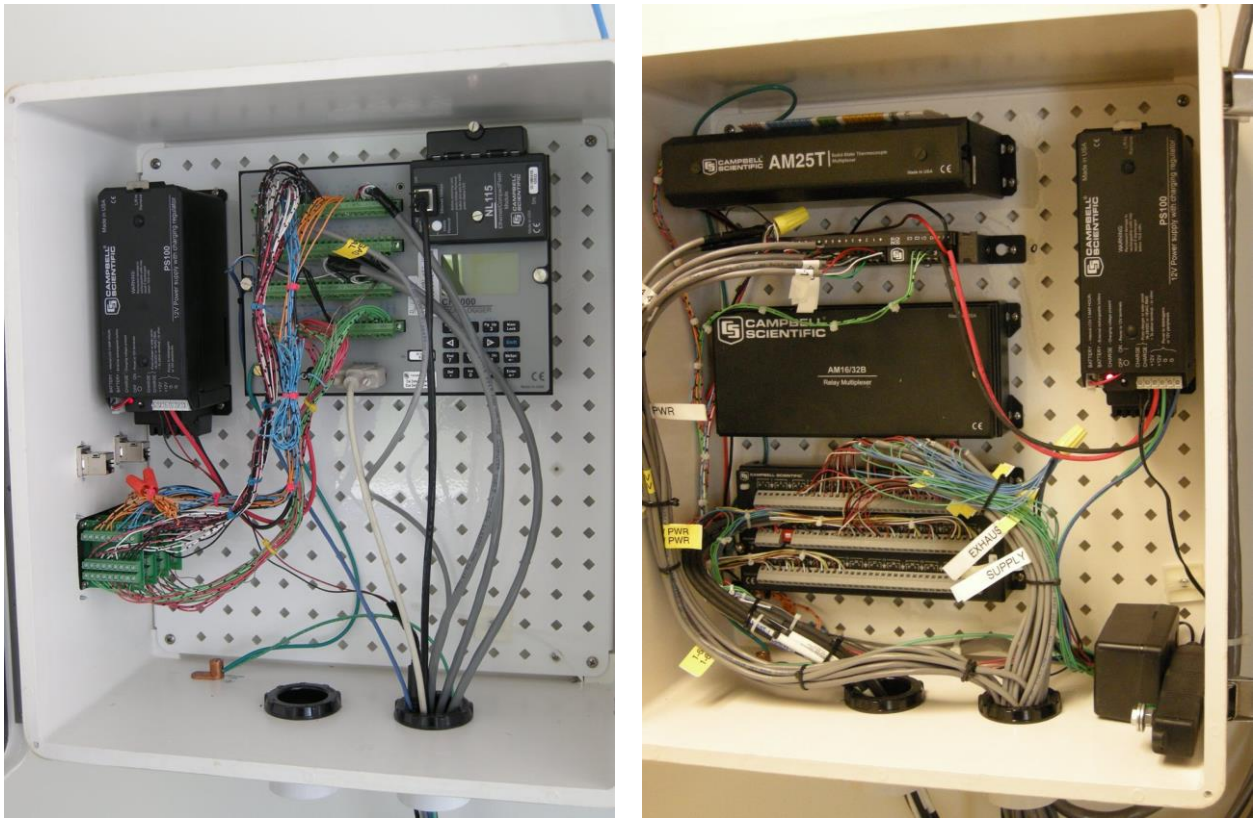

Fig. 10. CR 3000 data logger.

Fig. 11. Supply air temperature and RH sensor for wall unit.

Fig. 12. Supply and return air temperature and RH sensors for VRF ceiling unit.

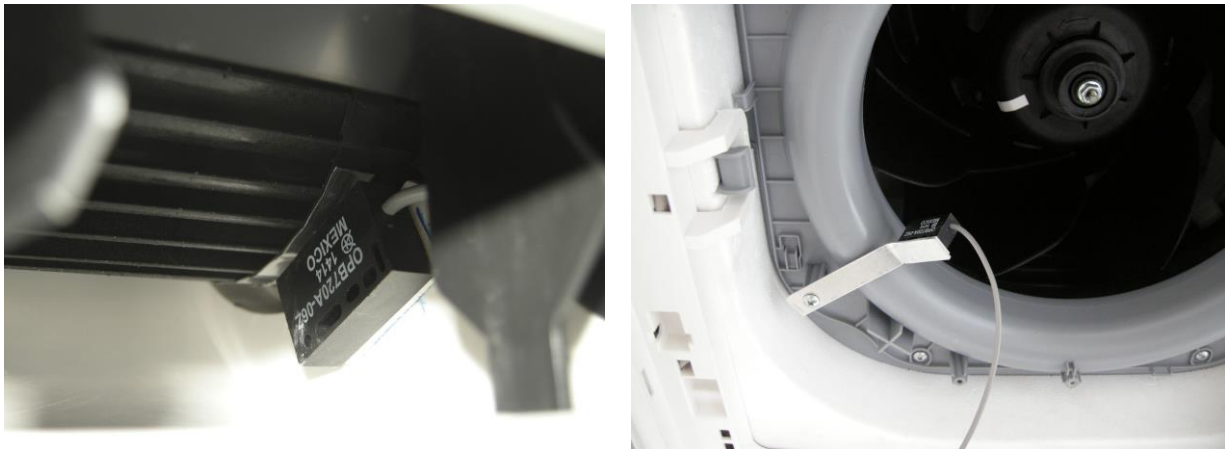

Fig. 13. Fan speed sensor for VRF wall-mounted (left) and ceiling unit (right).

4.2 Monitoring Plan

To evaluate the performance of the VRF system and the CCM control, three HVAC system/control scenarios were applied to the FRP:

1. Baseline RTU with thermostat-only control (RTU)
   The first scenario is a baseline case with conventional thermostatic control. The RTU system is controlled with a central energy management system (EMS) with cooling and heating schedules. Table 4 shows the thermostat schedule for the baseline. There is no separate weekday/weekend schedule.
2. VRF system with thermostat-only control (VRF–thermostat)
   The second scenario is a VRF system with the same thermostatic schedule as scenario 1. Because this system is a heat pump model and no simultaneous heating and cooling is possible, the heating and cooling modes were switched manually.[2]
3. VRF system with CCM control (VRF–CCM)
   The VRF system was operated with CCM control. The enhanced control (CCM) was developed to control the indoor condition based on not only temperature but also RH and indoor airflow.

The RTU, VRF–thermostat, and VRF–CCM were operated alternately for weeklong periods by switching the system and controls according the schedule shown in Table 5.

Table 4. Thermostat schedule

	During occupied hours (6 a.m. – 6 p.m.)	**During unoccupied hours (6 p.m. – 6 a.m.)**
Cooling	24°C	30°C
Heating	21°C	15.5°C

Table 5. HVAC system operation schedule (June 2014 through February 2015)

Jun 2014		Jul 2014				Aug 2014					Sep 2014			
Week 3	Week 4	Week 1	Week 2	Week 3	Week 4	Week 1	Week 2	Week 3	Week 4	Week 5	Week 1	Week 2	Week 3	Week 4
RTU	VRF-Tstat	VRF-CCM	RTU	VRF-Tstat	VRF-CCM	RTU	VRF-Tstat	VRF-CCM	RTU	VRF-Tstat	VRF-CCM	RTU	VRF-Tstat	VRF-CCM
Oct 2014					Nov 2014				Dec 2014					Jan 2015
Week 1	Week 2	Week 3	Week 4	Week 5	Week 1	Week 2	Week 3	Week 4	Week 1	Week 2	Week 3	Week 4	Week 5	N/A[3]
RTU	VRF-Tstat	VRF-CCM	RTU	VRF-Tstat	VRF-CCM	RTU	VRF-Tstat	VRF-CCM	RTU	VRF-Tstat	VRF-CCM	RTU	VRF-Tstat	
Jan 2015			Feb 2015											
Week 2	Week 3	Week 4	Week 1	Week 2	Week 3	Week 4								
VRF-CCM	RTU	VRF-Tstat	VRF-CCM	RTU	VRF-Tstat	VRF-CCM								

[2] Later in October 2014, a new algorithm was implemented to switch the heating and cooling mode by a master thermostat located in room 106.

[3] The CCM algorithm was updated during the first week of January, and the data are not valid for the period.

4.3 Analysis Plan

The performance of the VRF system was analyzed in terms of the energy use, ability to maintain indoor temperatures, and ability to provide thermal comfort. These performance parameters were evaluated for both the VRF–thermostat and VRF–CCM systems against the baseline RTU system. The analyses were performed separately for the cooling and heating seasons. For the annual energy analysis, calibrated building energy simulation was performed.

4.3.1 HVAC Energy Consumption Analysis

Since the emulated occupancy was unchanged throughout the study, variations in the energy use are attributable only to system performance and weather. This allowed for weather-normalization of the energy use and a high-level comparison of energy use among different systems/controls. Since the systems/controls were operated alternately during the measurement period, inverse models of the energy use were developed using the measured data, which allowed a precise comparison of the systems' energy performance at varying OA temperatures. These models were also used for estimating the energy use for the entire measurement period.

4.3.2 Thermal Comfort Analysis

The performance of the systems was compared in terms of maintaining the indoor temperature. To accomplish this, the measured hourly indoor temperatures in each of the ten thermal zones were compared with the thermostat settings to see if the system could provide adequate cooling and heating to the zones. In addition, the ability of the systems/controls to maintain thermal comfort was compared using the Predicted Mean Vote/Predicted Percentage of Dissatisfied (PMV/PPD) method (ASHRAE 2013). The PMV/PPD model provides two thermal comfort indices defined by six parameters: air temperature, mean radiant temperature, RH, air speed, metabolic rate, and clothing insulation. PMV represents occupants' thermal sensations on a 7-point scale from cold (−3) to hot (+3), with zero as the ideal value representing thermal neutrality. PPD represents the percentage of occupants satisfied with the indoor conditions. ASHRAE Standard 55-2013 (ASHRAE 2013) specifies criteria for acceptable thermal comfort as $-0.5 < PMV < +0.5$, and $PPD < 10$.

For each system/control in this study, the PMV and PPD were calculated for each zone using the measured hourly air temperature, mean radiant temperature, and RH, along with the assumptions about the air speed, metabolic rate, and clothing insulation shown in Table 6. Inferences about the ability of the systems to provide thermal comfort were made by statistically analyzing the PMV and PPD values against ASHRAE Standard 55 criteria for acceptable thermal comfort.

Table 6. Key assumptions for PMV/PPD analysis

	Summer operation	Winter operation
Indoor velocity	15 fpm	15 fpm
Clothing level	0.7 clo	1.0 clo
Activity level	1.0 met	1.1 met

5. COOLING SEASON DATA ANALYSIS

This chapter discusses the cooling season data analysis of the RTU, VRF–thermostat, and VRF–CCM systems/controls. The analysis is based on the measured data from July 7 through September 30, 2014 (i.e., 12 weeks and 3 days), during which time the three systems were switched according to the schedule shown in Table 5. The zone thermostatic settings were 24°C during the occupied hours (i.e., 6 a.m. to 6 p.m.) and 30°C during the unoccupied hours. The building was operated with preprogrammed occupancy and lighting schedules as described in Section 2.2.

During summer 2014, certain anomalies found in the building and system operation and measured data were handled in the analysis as follows:

1. Based on the RTU refrigerant-side analysis, it was suspected that the refrigerant in condenser circuit 1 had been low. The refrigerant in circuit 1 was recharged on September 30, 2014. The measured data after the charge showed lower RTU cooling energy consumption. Further investigation revealed that the refrigerant might have leaked while the RTU was turned off during the VRF system installation. Therefore, the RTU cooling energy use data during the analysis period was discarded and the summer 2013 data were used for the analysis instead.
2. During summer 2013, the thermostat settings did not have a setback, as opposed to the 6°C night setback applied in summer 2014. Therefore, the RTU cooling energy use during the system startup at 6 a.m. in summer 2014 was usually higher because of the system's response to quickly recover from the unoccupied mode. Therefore, the measured data from 6 a.m. to 8 a.m. were excluded from the analysis to exclude the hours with potentially different system behaviors in terms of startup effects.
3. During RTU operation in the summer, the VAV zone reheat energy use was very small (almost constant) and was inadequate for detecting any temperature-dependent variation. Therefore, to determine the reheat energy use as a function of OA temperature, a shoulder month was preferred that had notable variation in the reheat energy use. Thus, for analyzing the measured zone reheat energy use, October 2014 data were used.
4. During August 8, 2014, through the cooling season, construction was taking place inside the FRP. Although the workers were informed about the experiment and provided with instructions to prevent disruption of the experiment, the measured data during the construction were suspected to have more noise/outliers than the data before the construction. Therefore, any anomalies in the data during the construction period were excluded in this analysis.

To summarize, the energy analysis for the three systems was performed using hourly data from 8 a.m. to 6 p.m. on the weekdays. The energy analysis of the VRF–thermostat and VRF–CCM is based on the measured data during July 7 through September 30, 2014. For the RTU energy analysis, the cooling energy analysis is based on August–September 2013 measured data, and the VAV reheat energy analysis is based on October 2014 measured data. Using the best-fit models for measured energy use data, energy use for the entire cooling season was estimated for each system.

5.1 HVAC Energy Consumption Analysis

5.1.1 RTU Hourly Energy Use

The total RTU energy use is the sum of the RTU cooling energy use (which includes the compressor, condenser fan, and supply fan energy use) and the VAV zone reheat energy use. The RTU cooling energy use was analyzed using the September 2013 measured data. The VAV reheat energy use was analyzed using the October 2014 measured data for those days when the RTU was operating. Fig. 14 shows the scatter-plot of the hourly RTU cooling energy use versus the OA temperature (T_{OA}) for occupied hours in September 2013. Fig. 15 shows the scatter-plot of the hourly VAV reheat energy use versus the T_{OA} during the occupied hours in October 2014. From the scatter-plots, the best-fit models for the RTU cooling energy use and VAV reheat energy use were generated (as shown in Eqs. [1] and [2]) and used to estimate the total RTU energy use for all weekdays during the July 7 through September 30, 2014 period.

$$RTU\ cooling\ energy\ use\ (Wh) = 1.3494 * {T_{OA}}^2 + 191.95 * T_{OA} + 1370.2\ . \quad (1)$$

$$VAV\ reheat\ energy\ use\ (Wh) = \begin{cases} -0.0129 * {T_{OA}}^4 - 0.6756 * {T_{OA}}^3 + 83.351 * {T_{OA}}^2 - 2115.2 * T_{OA} + 16647, for\ T_{OA} < 20℃ \\ 190, otherwise \end{cases} \quad (2)$$

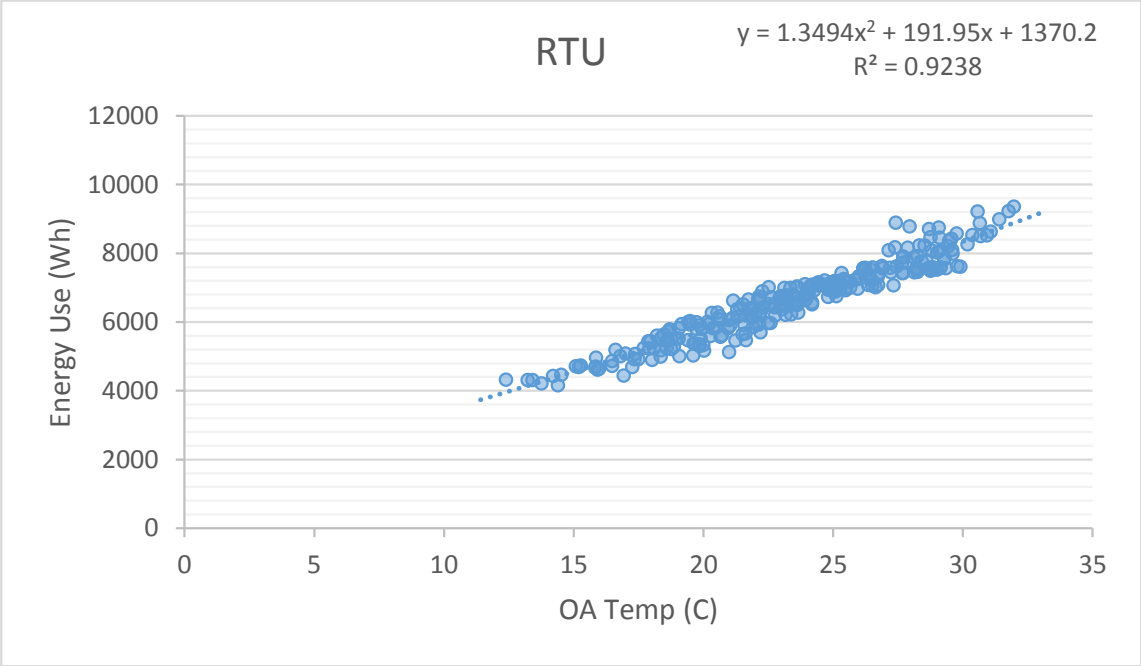

Fig. 14. Measured hourly RTU cooling energy use (September 2013).

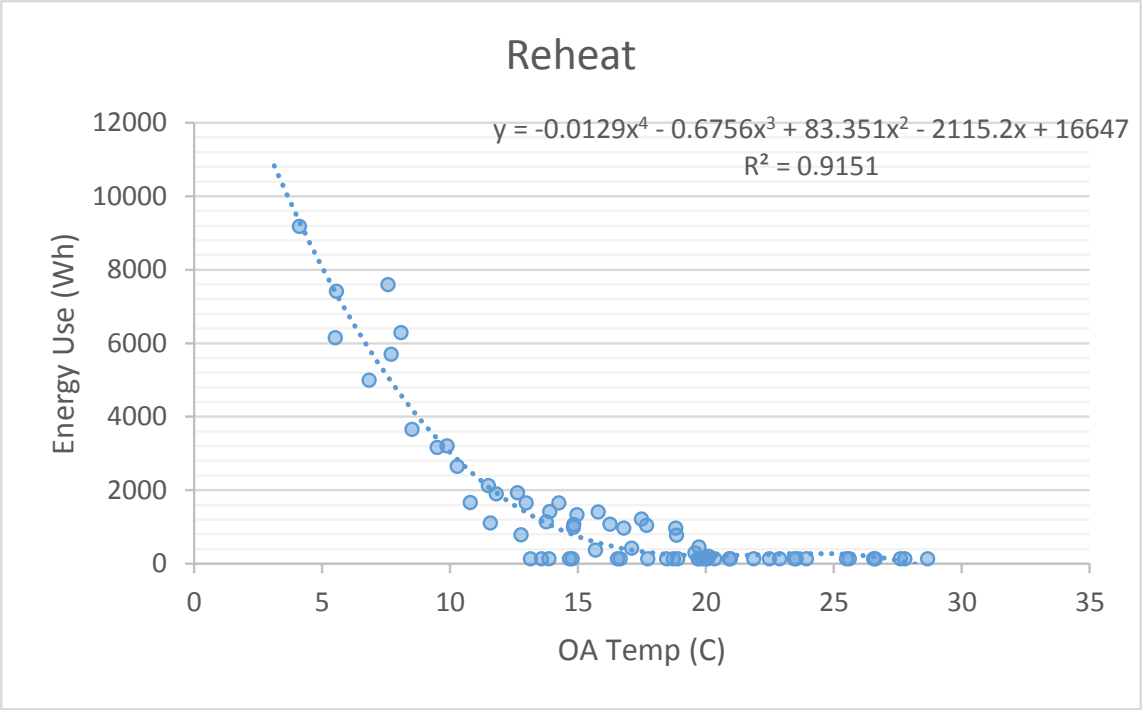

Fig. 15. Measured hourly RTU VAV reheat energy use (October 2014).

5.1.2 VRF–Thermostat Hourly Energy Use

The VRF energy use includes the energy use of the outdoor unit and ten indoor units. The VRF–thermostat energy use was analyzed using the measured data from July 7 through September 30, 2014 for those days when the VRF–thermostat was operating. The hourly VRF energy use during occupied hours was filtered and plotted as a function of OA temperature (T_{OA}), as shown in Fig. 16. From this scatter-plot, the best-fit model for the VRF energy use was generated (as shown in Eq. [3]) and used to estimate the VRF–thermostat energy use for all weekdays during the July 7 through September 30, 2014 period.

$$VRF\_Thermostat\ energy\ use\ (Wh) = 4.0813 * {T_{OA}}^2 + 152.73 * T_{OA} + 91.872\ . \quad (3)$$

5.1.3 VRF–CCM Hourly Energy Use

The same approach used for VRF–thermostat was used to calculate the energy use for those weekdays when the VRF–CCM was operating. Fig. 17 shows the scatter-plot for hourly VRF–CCM energy use. From the scatter-plot, the best-fit model for the VRF–CCM energy use was generated (as shown in Eq. [4]) and used to estimate the total VRF–CCM energy use for all weekdays during the July 7 through September 30, 2014 period.

$$VRF\_CCM\ energy\ use\ (Wh) = 3.7501 * {T_{OA}}^2 + 195.32 * T_{OA} - 1339.3\ . \quad (4)$$

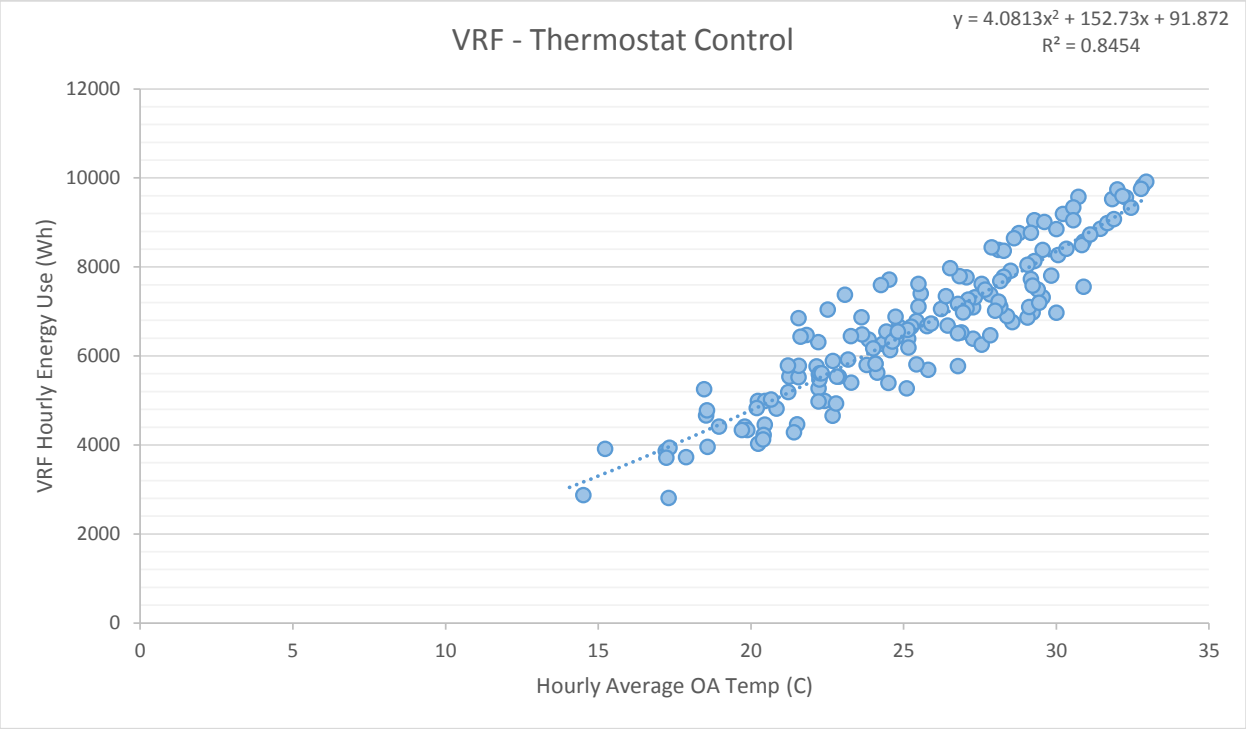

Fig. 16. Measured hourly VRF–thermostat energy use (July 7 through September 30, 2014).

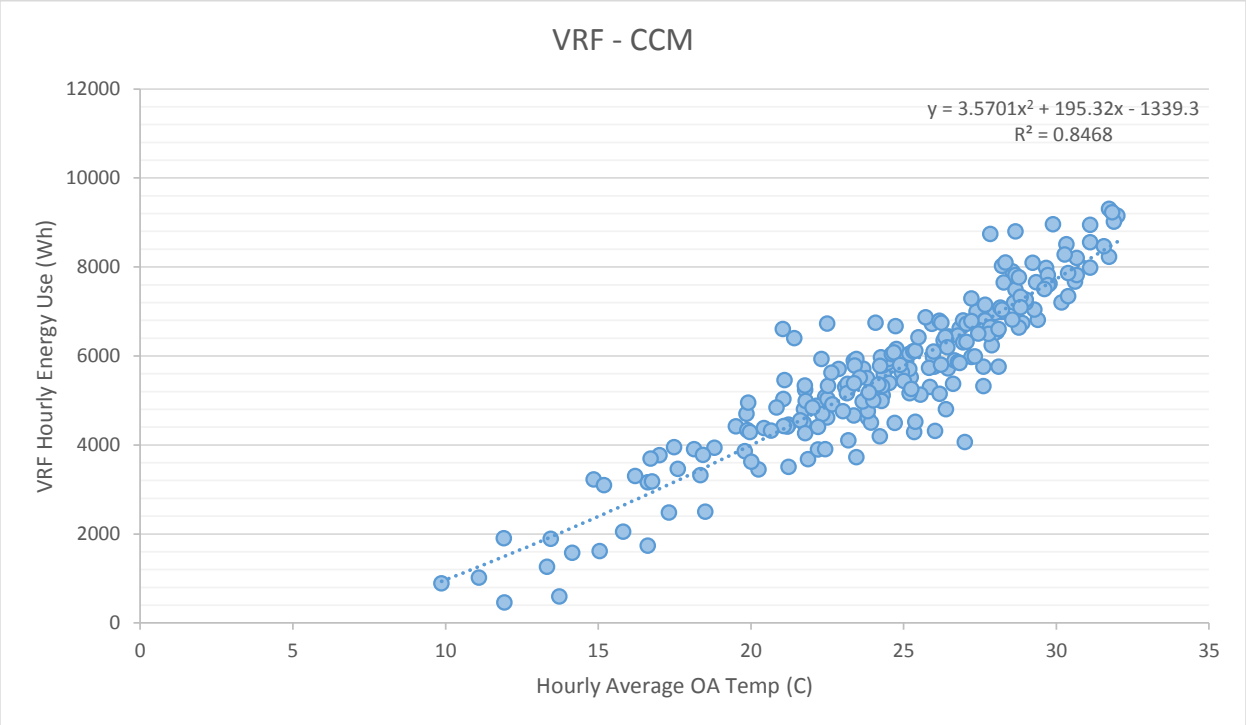

Fig. 17. Measured hourly VRF–CCM energy use (July 7 through September 30, 2014).

5.1.4 Energy Use Comparison

Fig. 18 compares the best-fit models developed for the hourly energy consumption for the RTU, VRF–thermostat, and VRF–CCM considering the occupied hours only. Compared with the RTU, the VRF system uses significantly less energy at lower OA temperatures. The difference in the RTU and VRF energy use diminishes at higher OA temperatures approaching 30°C. This finding was expected because of the better part-load cooling performance of the VRF system at moderate OA temperatures. At temperatures below 15°C, the RTU system energy use increases because of the VAV reheat energy use.[4] Compared with the VRF–thermostat, the VRF–CCM almost consistently used less energy for the entire OA temperature range observed.

To comprehend the scale of these differences in the energy use, they are also plotted in Fig. 18. Compared with the RTU, HVAC energy savings can reach up to 20% for the VRF–thermostat and up to 32% for the VRF–CCM at a 20°C OA temperature. When comparing the VRF–thermostat to the VRF-CCM, the HVAC energy savings can reach up to 19% for the VRF-CCM at a 20°C OA temperature, which drops to about 4.5 % savings at a 32°C OA temperature.

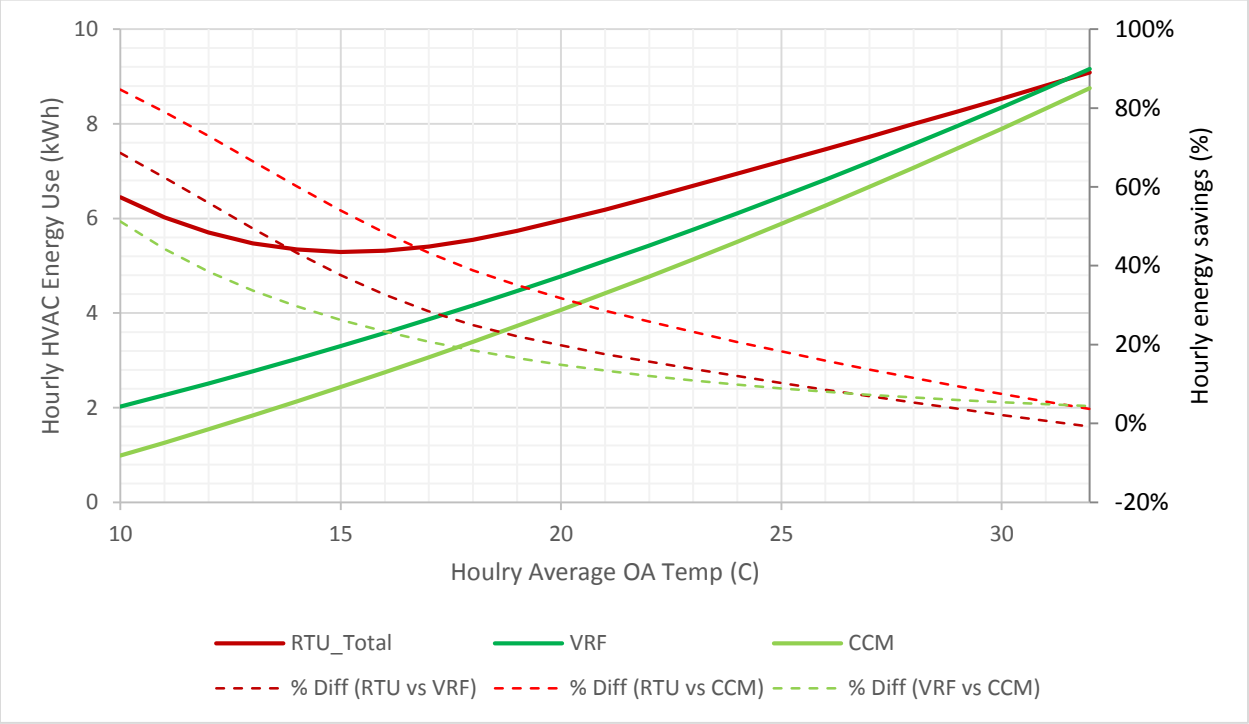

Fig. 18. Modeled hourly energy use for RTU, VRF-thermostat, and VRF-CCM.

[4] In this study, the RTU was consistently providing supply air at 14°C, which needed to be reheated when the zone temperature was below 21°C. If the outdoor reset or seasonal reset schedule were applied to the RTU, the cooling and reheat energy consumption would be reduced during the shoulder and heating seasons.

In addition to the better performance of the VRF system during the occupied period, there were significant differences in the energy use during the unoccupied hours. During the analysis period, the RTU unit used, on average, 900 W during unoccupied hours, with most of this attributed to the fan for circulating the air. In contrast, the VRF system with thermostat control and CCM control used only 330W and 240W, on average, respectively. Thus, accounting for the unoccupied hours, the energy savings from the VRF system were even higher, compared with the RTU system. Table 7 compares the total energy use of these systems for weekdays considering (a) the occupied hours (8 a.m. to 6 p.m.), and (b) the 24 hour period. Considering only the occupied hours, the VRF–thermostat and VRF–CCM used 11% and 19% less energy, respectively, than the RTU. The VRF–CCM used about 9% less energy than the VRF–thermostat. Accounting for the unoccupied periods, the VRF–thermostat and VRF–CCM saved about 17% and 26% in energy use, respectively, compared with the RTU. The VRF–CCM used about 10% less energy than the VRF–thermostat.

Table 7. HVAC energy use during weekdays (July 7 through September 30, 2014)

	Accounting for occupied hours (8 a.m. – 6 p.m.)			Accounting for 24 hours		
	Energy use (kWh)	Difference vs. RTU (%)	Diff. vs. VRF–thermostat (%)	Energy use (kWh)	Diff. vs. RTU (%)	Diff vs. VRF–thermostat (%)
RTU	4,910	–	–	5,635	–	–
VRF–thermostat	4,395	10.5%	–	4,661	17.3%	–
VRF–CCM	3,996	18.6%	9.1%	4,189	25.7%	10.1%

5.2 Thermal Comfort Analysis

The performance of each system/control in maintaining the indoor temperatures and providing thermal comfort in each of the ten thermal zones was evaluated as described below.

5.2.1 Indoor Temperature

Fig. 19 presents the indoor temperature statistics for the RTU, VRF–thermostat, and VRF–CCM.

- The median zone temperatures for RTU operation show that the first floor zones were slightly overcooled.
- For both VRF–thermostat and VRF–CCM, the median zone temperature for rooms 202 and 203 was much higher (~2–3°C higher) than the thermostat setting. During the VRF system commissioning, the indoor unit in room 203 was found to be malfunctioning —overheating and turning off. To prevent that, the maximum fan CFM volume was reduced manually by Samsung. In addition, recent CFM measurements showed that the measured CFM volume for rooms 202 and 203 was much lower than the manufacturer's specification. Therefore, it is possible that the systems in rooms 202 and 203 were unable to provide adequate cooling.
- For the VRF–CCM, the maximum temperature in rooms 105, 106, 204, and 206 reached almost to 30°C, which could be uncomfortable for most occupants. Further updating of the algorithm is needed to improve the thermal comfort in such zones. Three of these rooms are southeast- and southwest-facing perimeter zones, which have higher solar heat gains.

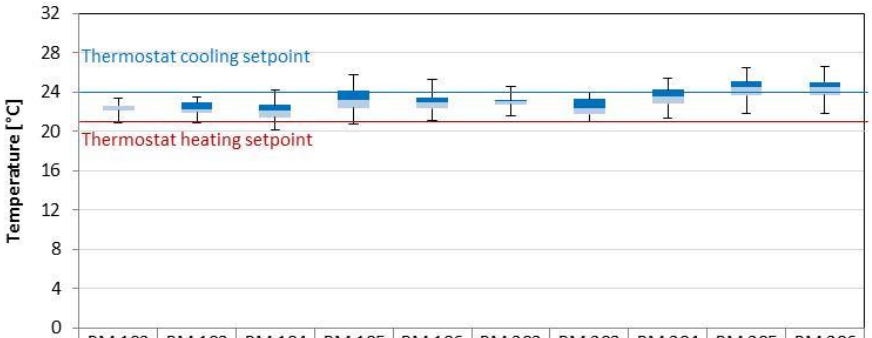

	RM 102	RM 103	RM 104	RM 105	RM 106	RM 202	RM 203	RM 204	RM 205	RM 206
Max	23.38	23.51	24.25	25.81	25.27	24.54	24.00	25.43	26.47	26.64
Q3	22.66	22.93	22.68	24.18	23.49	23.21	23.28	24.24	25.08	25.02
Median	22.58	22.32	22.15	23.26	22.92	23.05	22.41	23.55	24.49	24.58
Q1	22.16	21.93	21.44	22.44	22.32	22.78	21.74	22.83	23.64	23.73
Min	20.84	20.84	20.19	20.76	21.08	21.56	21.04	21.38	21.86	21.88

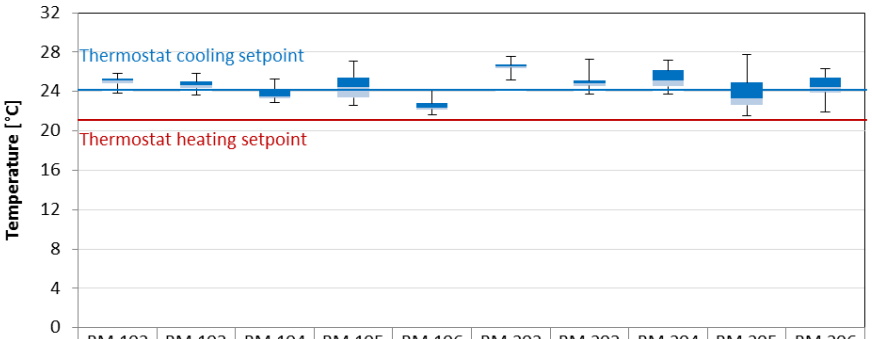

	RM 102	RM 103	RM 104	RM 105	RM 106	RM 202	RM 203	RM 204	RM 205	RM 206
Max	25.84	25.83	25.24	27.11	24.09	27.61	27.29	27.17	27.78	26.31
Q3	25.31	25.03	24.15	25.44	22.83	26.72	25.12	26.15	24.91	25.46
Median	25.10	24.68	23.54	24.48	22.38	26.58	24.82	25.08	23.33	24.49
Q1	24.84	24.36	23.32	23.40	22.19	26.37	24.57	24.54	22.64	23.92
Min	23.88	23.60	22.89	22.56	21.67	25.13	23.74	23.77	21.51	21.94

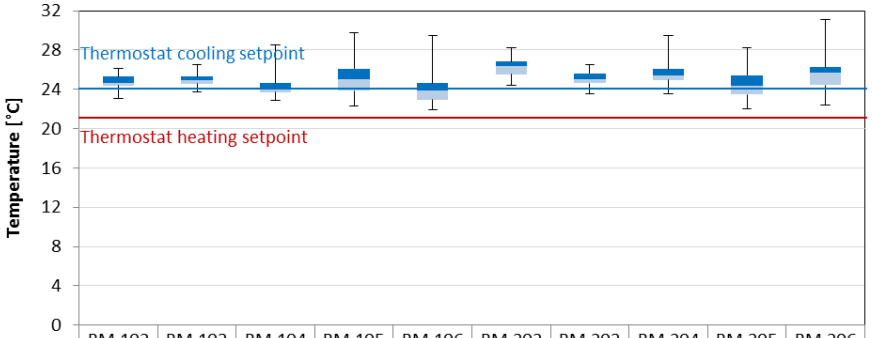

	RM 102	RM 103	RM 104	RM 105	RM 106	RM 202	RM 203	RM 204	RM 205	RM 206
Max	26.13	26.52	28.56	29.78	29.44	28.22	26.55	29.44	28.22	31.11
Q3	25.29	25.29	24.62	26.09	24.63	26.83	25.61	26.06	25.42	26.25
Median	24.64	24.90	24.08	25.00	23.92	26.38	25.05	25.38	24.39	25.72
Q1	24.36	24.59	23.74	23.86	22.96	25.52	24.62	24.96	23.48	24.44
Min	23.09	23.72	22.90	22.35	21.91	24.37	23.53	23.55	22.04	22.44

Fig. 19. Cooling season zone temperature by room for (a) RTU, (b) VRF–thermostat, and (c) VRF–CCM.

5.2.2 PMV/PPD Values

Further analysis of the indoor thermal conditions was performed using the PMV/PPD method. PMV and PPD values for each of the ten zones were calculated and compared. The PMV range between −0.5 and 0.5 and PPD <10 is considered acceptable for thermal comfort. PMV values greater than 0.5 indicate a warm/hot thermal sensation, whereas PMV values less than −0.5 indicate a cool/cold thermal sensation.

The hourly PMV/PPD values for each room with the three HVAC modes are shown in Fig. 20 through Fig. 22. The data show clearly that, for the RTU, all rooms without a southern exposure had PVM values below 0 for almost all hours and beyond the −0.5 limit for most hours, indicating that these rooms would generally feel too cold to many occupants (PPD shown on the y-axis). Rooms with southern exposure were no different, except for a few hours when the PMV was above 0. However, the PMV values rarely exceeded 0.5, which confirms that the only possible concern during RTU system operation would be that rooms were too cold. PMV values for VRF–thermostat were within the acceptable range most of the time (note that because of an issue with the mean radiant temperature (MRT) measurement, only a small set of useful thermal performance data was available for VRF–thermostat). Only the southern exposure rooms had a few PMV values beyond −0.5 and 0.5. VRF–CCM PMV values show varying thermal comfort trends in different rooms. The non–south facing rooms were too warm at times, whereas the south-facing rooms were too warm at some times and too cold at other times.

The PMV statistics in Fig. 23 provide a quantitative summary of the thermal comfort conditions. The PMV values for RTU tend to be lower than the values for VRF–thermostat and VRF–CCM, indicating that the RTU system was slightly overcooling the rooms, particularly first-floor rooms. Since both systems are controlled by the same thermostat settings, further investigation is needed to identify the causes of the discrepancies. Possible causes include uncalibrated thermostats, different thermostat dead bands, or different control algorithms. VRF–CCM PMV values had a wide range, meaning that the comfort conditions in the rooms were variable; it would require further investigation to better provide comfort conditions.

Table 8 shows the median PMV values for each room. Table 9 shows the percentage of hours when PMV values were below −0.5 (cool/cold sensation), between −0.5 and 0.5 (acceptable thermal comfort), and above 0.5 (warm/hot sensation). As shown in Table 9, the VRF–thermostat and VRF–CCM scenarios were able to meet the acceptable thermal comfort criteria for more than 70% of total operating hours, whereas the RTU system could meet the thermal comfort criteria for only 45% of total operating hours.

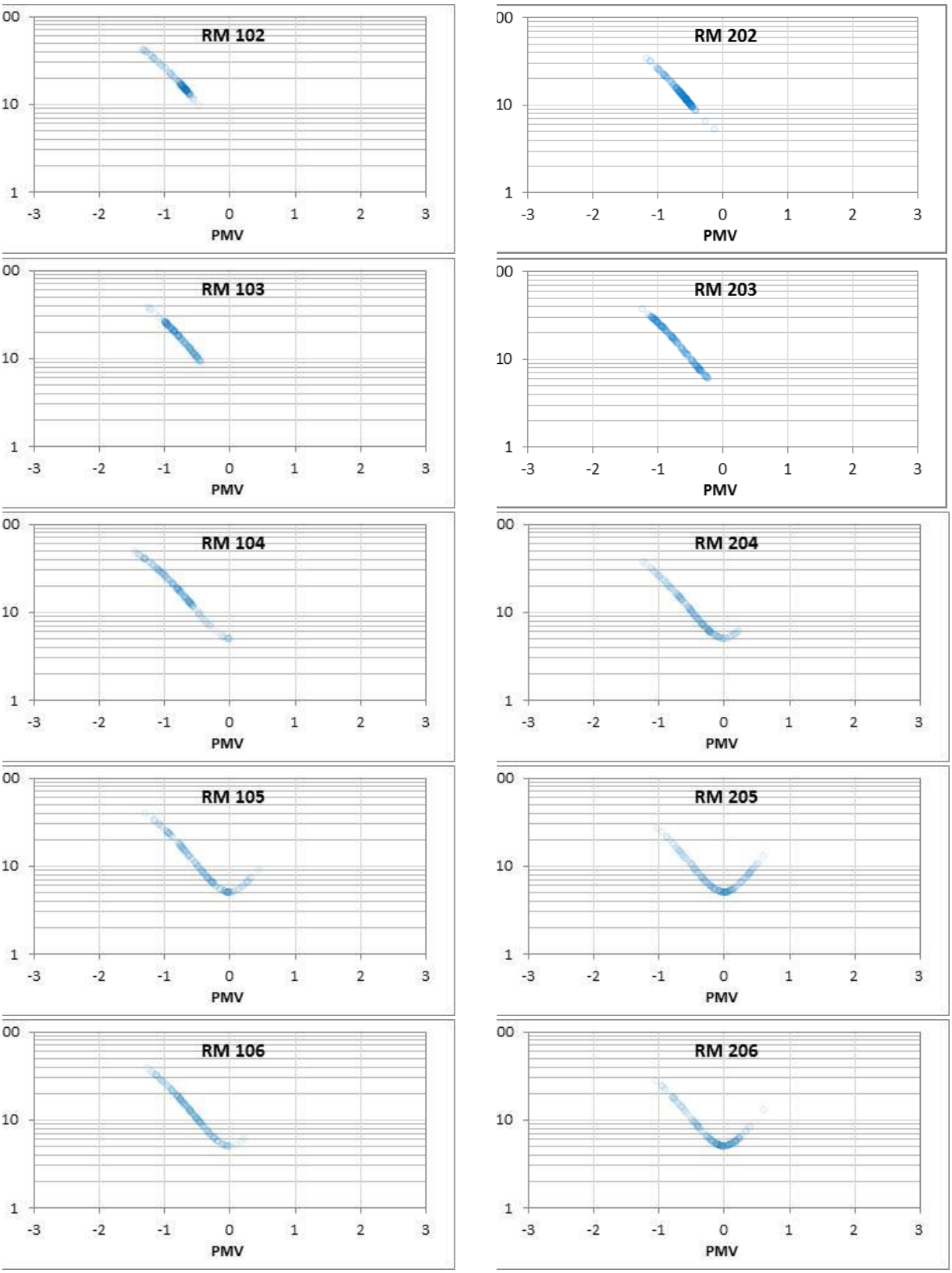

Fig. 20. Cooling season PMV values by room for RTU.

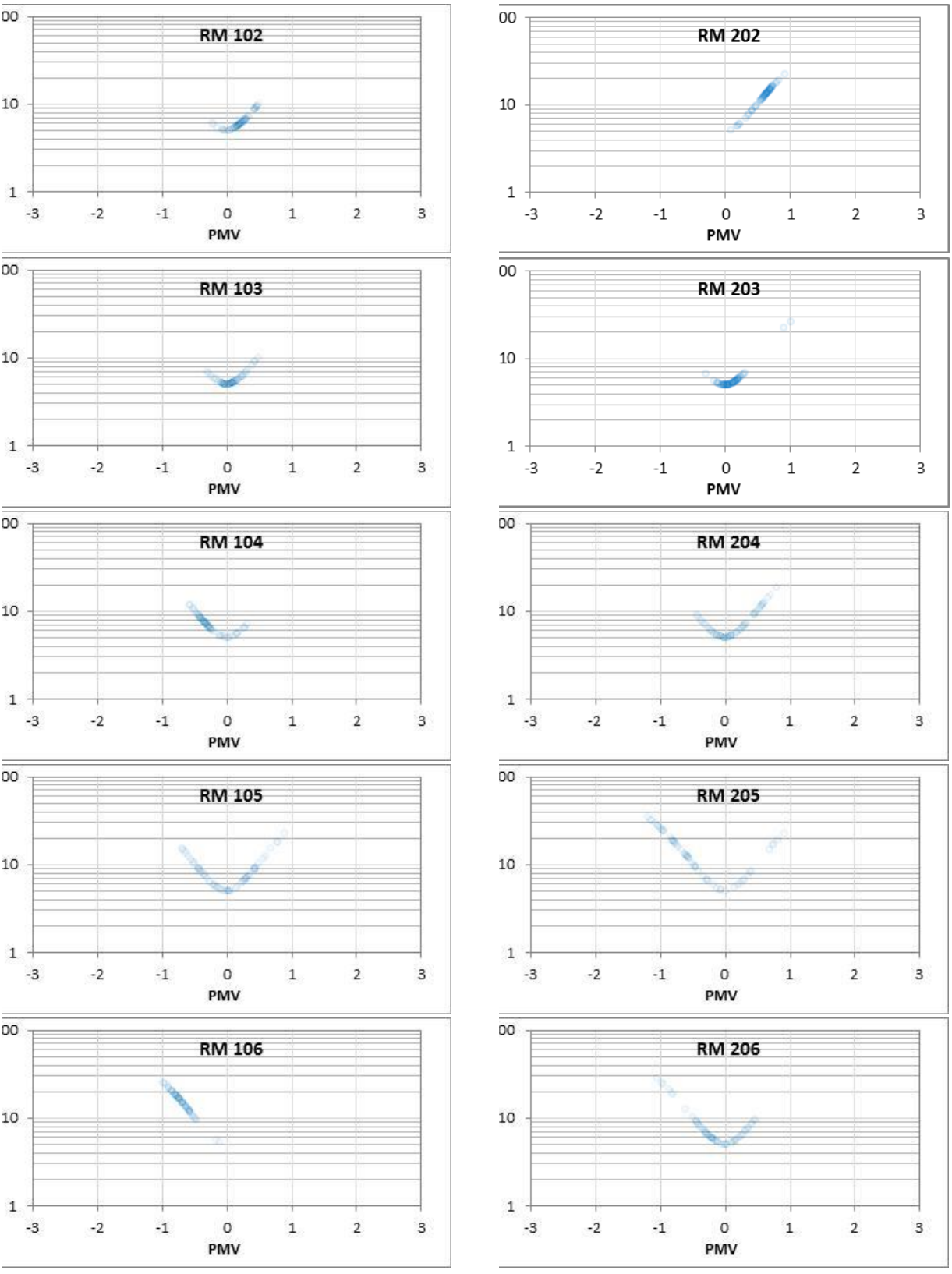

Fig. 21. Cooling season PMV/PPD values by room for VRF–thermostat.

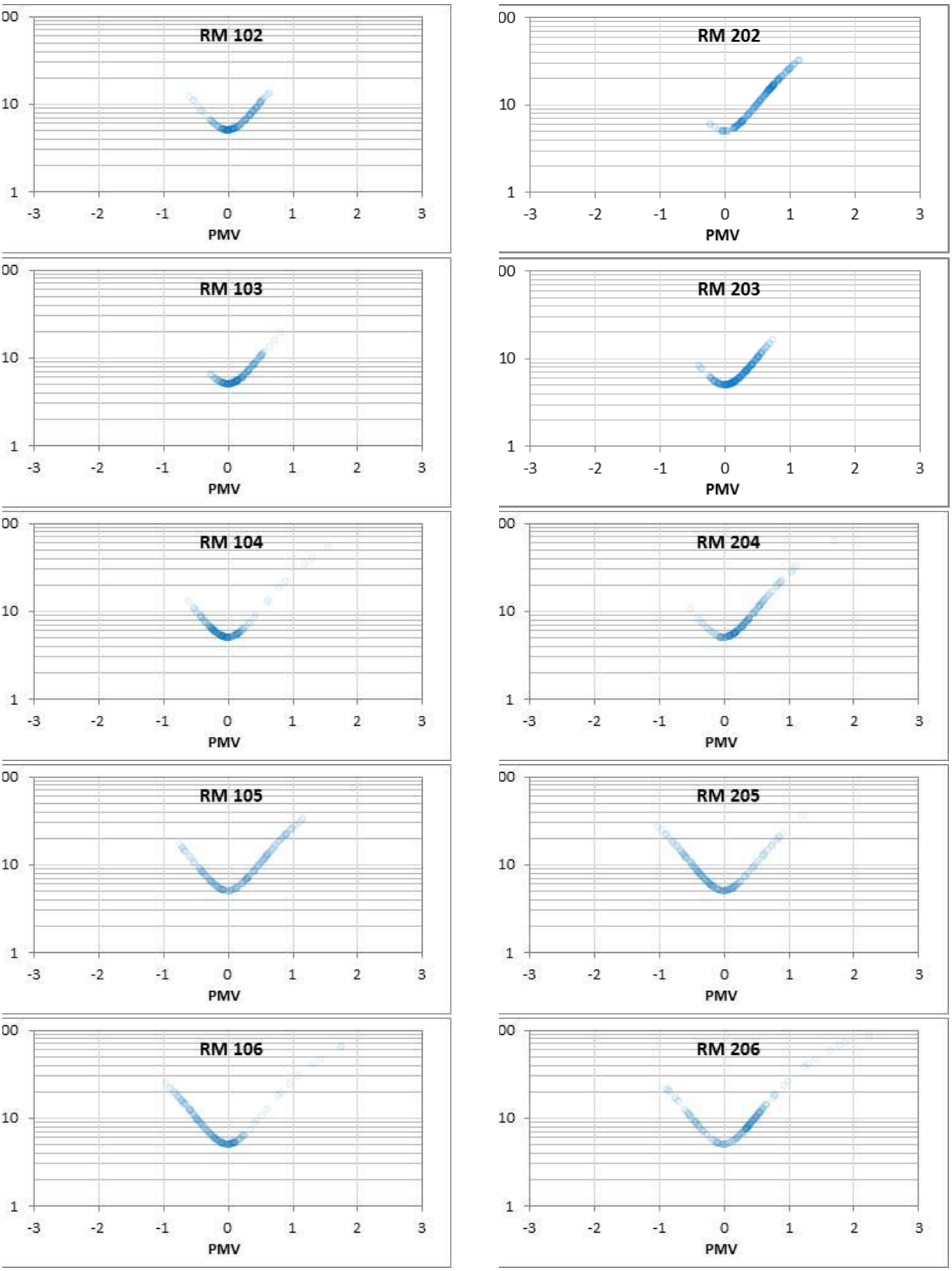

Fig. 22. Cooling season PMV/PPD values by room for VRF–CCM.

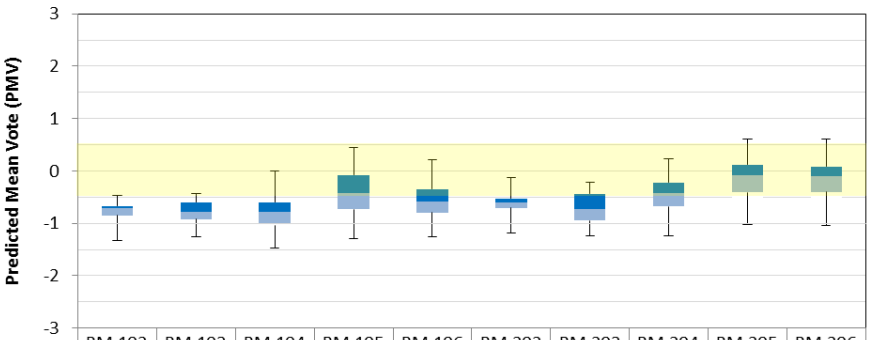

	RM 102	RM 103	RM 104	RM 105	RM 106	RM 202	RM 203	RM 204	RM 205	RM 206
Max	-0.46	-0.43	0.00	0.44	0.22	-0.12	-0.22	0.23	0.61	0.61
Q3	-0.66	-0.60	-0.59	-0.08	-0.34	-0.53	-0.43	-0.22	0.12	0.08
Median	-0.71	-0.78	-0.78	-0.41	-0.59	-0.60	-0.73	-0.42	-0.08	-0.10
Q1	-0.85	-0.92	-1.03	-0.73	-0.79	-0.71	-0.95	-0.68	-0.41	-0.40
Min	-1.34	-1.25	-1.47	-1.29	-1.25	-1.18	-1.24	-1.24	-1.02	-1.03

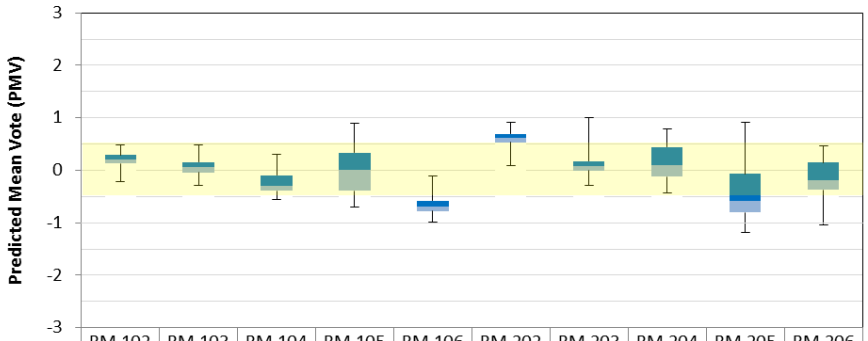

	RM 102	RM 103	RM 104	RM 105	RM 106	RM 202	RM 203	RM 204	RM 205	RM 206
Max	0.48	0.48	0.31	0.90	-0.11	0.92	1.01	0.79	0.91	0.46
Q3	0.29	0.15	-0.10	0.33	-0.58	0.69	0.17	0.44	-0.07	0.15
Median	0.20	0.06	-0.31	0.00	-0.70	0.63	0.08	0.09	-0.57	-0.19
Q1	0.13	-0.05	-0.39	-0.39	-0.78	0.53	-0.01	-0.12	-0.80	-0.37
Min	-0.23	-0.30	-0.56	-0.69	-0.98	0.09	-0.29	-0.44	-1.19	-1.04

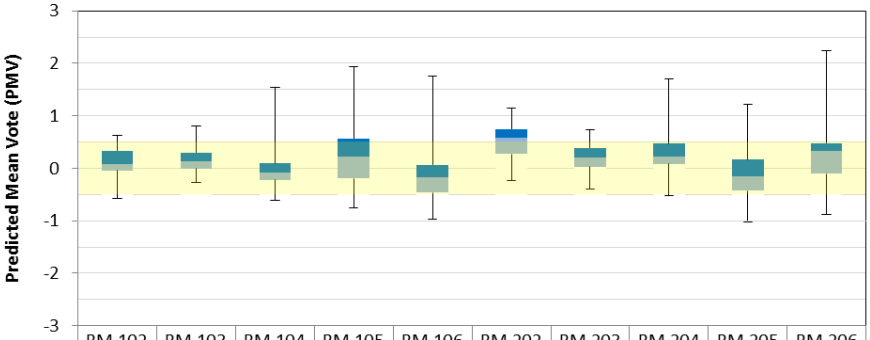

	RM 102	RM 103	RM 104	RM 105	RM 106	RM 202	RM 203	RM 204	RM 205	RM 206
Max	0.63	0.81	1.55	1.94	1.75	1.15	0.74	1.71	1.21	2.24
Q3	0.33	0.30	0.10	0.57	0.07	0.75	0.39	0.47	0.16	0.48
Median	0.08	0.13	-0.09	0.22	-0.17	0.59	0.20	0.23	-0.16	0.34
Q1	-0.04	-0.01	-0.22	-0.19	-0.46	0.27	0.03	0.08	-0.43	-0.11
Min	-0.58	-0.27	-0.61	-0.75	-0.97	-0.23	-0.40	-0.52	-1.02	-0.88

Fig. 23. Cooling season PMV statistics by room for (a) RTU, (b) VRF–thermostat, and (c) VRF–CCM.

Table 8. Median PMV values by room for RTU, VRF–thermostat, and VRF–CCM

	RM 102	RM 103	RM 104	RM 105	RM 106	RM 202	RM 203	RM 204	RM 205	RM 206
RTU	−0.71	−0.78	−0.78	−0.41	−0.59	−0.60	−0.73	−0.42	−0.08	−0.10
VRF–thermostat	0.20	0.06	−0.31	0.00	−0.70	0.63	0.08	0.09	−0.57	−0.19
VRF–CCM	0.08	0.13	−0.09	0.22	−0.17	0.59	0.20	0.23	−0.16	0.34

Table 9. Percentage of operating hours meeting thermal comfort criteria

	Below −0.5 (Colder)	Between −0.5 and 0.5 (Comfort)	Above 0.5 (Warmer)
RTU	60.7%	39.0%	0.3%
VRF–thermostat	17.9%	70.6%	11.5%
VRF–CCM	6.3%	75.4%	18.3%

5.3 Performance during a Typical Summer Day

Fig. 24 shows the hourly RTU and VRF–thermostat energy consumption and room temperatures for a typical summer day.

- In general, both systems show similar patterns of energy use. Both systems show high energy use upon system startup at 6:00 a.m. to reach the new set point temperature (i.e., 24°C) quickly as the occupancy mode changes from “unoccupied” to “occupied.” Energy use decreased as the room temperature reached the set point temperature. However, the RTU used more energy (about 30% more than the VRF systems) during system startup.
- After the morning startup, the RTU system was able to reach the set point temperature, whereas with the VRF system, some rooms did not reach the set point temperature (rooms 202 and 203 in particular). It appears that the ceiling-mounted units provide better cooling capability.
- After the morning startup, the RTU slightly overcooled most rooms to about 21–23°C and then allowed the temperatures to gradually increase to 23 to 26°C until 6:00 p.m. The VRF system also provided cooling in the morning to reach the set point temperature. The starting temperature in the morning was about 22–25°C. It appears that the ceiling-mounted units in rooms 205 and 206 maintained the temperature close to the set point temperature throughout the day, whereas the wall-mounted units in rooms 202 and 203 could not provide enough cooling, particularly during the afternoon.

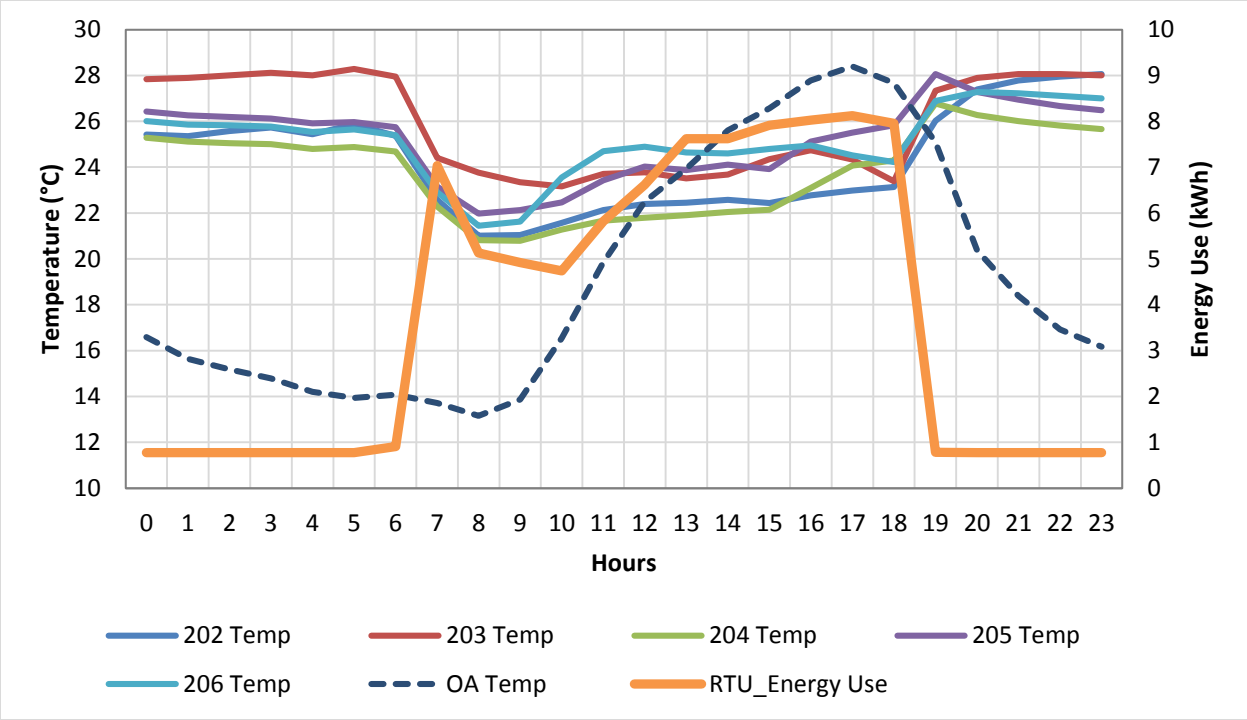

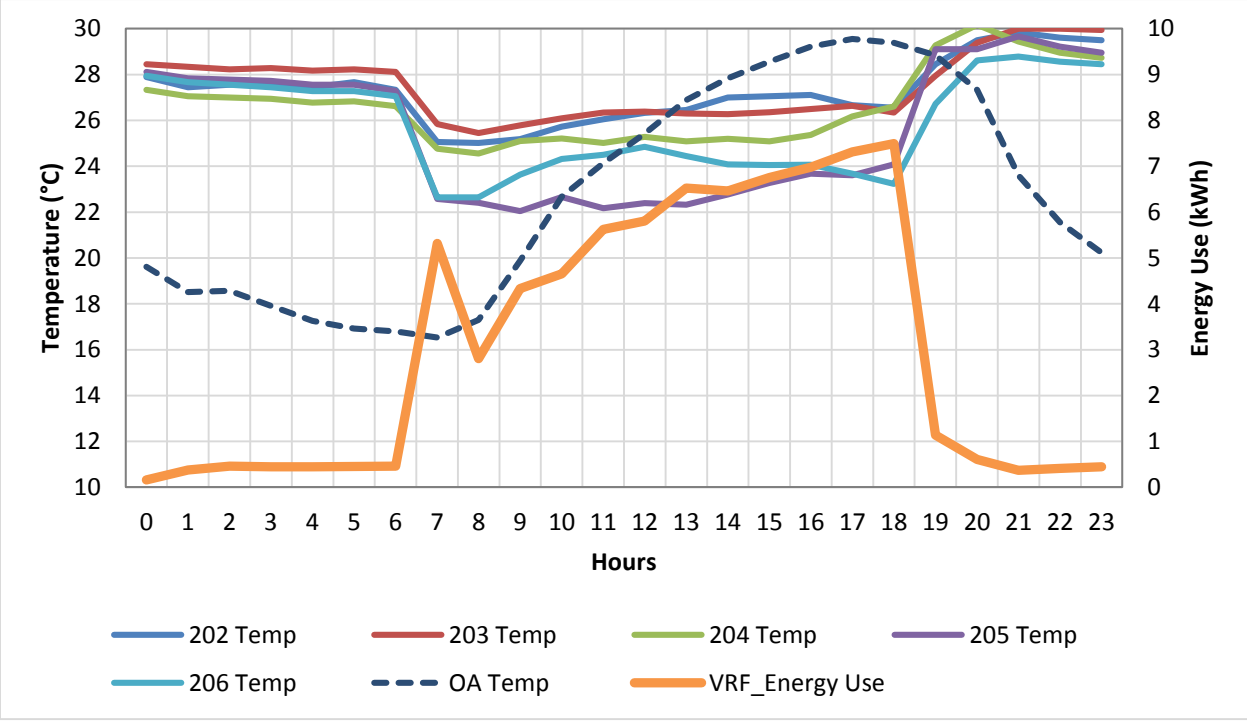

Fig. 24. Hourly energy consumption and room temperatures for a typical summer day for (a) RTU and (b) VRF systems.

6. HEATING SEASON DATA ANALYSIS

This chapter discusses a heating season data analysis for the RTU, VRF–thermostat, and VRF–CCM systems/controls. The analysis is based on the measured data from October 1, 2014 through February 28, 2015 (i.e., 21 weeks and 4 days) during which the three systems were switched according to the schedule shown in Table 5. The zone thermostat settings were 21°C during the occupied hours (i.e., 6 a.m. to 6 p.m.) and 15.5°C during the unoccupied hours. The building was operated with preprogrammed occupancy and lighting schedules, as described in Section 2.2.

The cooling season energy analysis was performed on an hourly basis because of an issue with the RTU system during summer 2014.[5] However, for the heating season, an energy analysis using daily total HVAC energy use was preferred, because the heating season data showed noticeable energy use during unoccupied hours even with the thermostat setback. Furthermore, the daily model did not show good correlation when only the OA temperature was used as the independent variable. Further investigation revealed that the building's heating loads were affected significantly by incident solar radiation, as well. This effect was likely due to the double-pane, clear glass windows without any internal or external shading. Therefore, a weather-normalized model of the energy use was developed with both the OA temperature and the global solar radiation as independent variables.

Since the analysis required a multi-variable regression model, the ASHRAE Inverse Modeling Toolkit (IMT) (Kissock et al. 2002) was used. ASHRAE's IMT is an application for calculating linear, change-point linear, variable-based degree-day, multi-linear, and combined regression models; and it is frequently used as a way of normalizing weather. The development of the IMT was sponsored by ASHRAE research project RP-1050 under the guidance of Technical Committee 4.7, Energy Calculations.

6.1 HVAC Energy Consumption Analysis

6.1.1 RTU Daily Energy Use

The daily total RTU energy use consists of RTU cooling energy use (i.e., compressor, condenser fan, and supply fan energy use) and the sum of the reheat energy use for ten zones. Fig. 25 shows a scatter-plot of daily total RTU energy use versus daily average OA temperature. While the RTU cooling energy use varied linearly with the daily average OA temperature (T_i), the reheat energy use did not show good correlation with the OA temperature (as discussed in Section 5). When the daily global solar radiation (S_i, W/m^2) was applied as a second independent variable (using the ASHRAE IMT), the model showed a better fit with the measured data. Equations (5) and (6) present the final model for the daily total RTU cooling energy use and the daily total reheat energy use, respectively, which are plotted in Fig. 25.

[5] As a result of RTU system refrigerant leakage in summer 2014, summer 2013 data were used. However, the summer 2013 operating schedule included no thermostat setback, whereas the summer 2014 schedule had a setback during unoccupied hours. So unoccupied hours had to be excluded from the analysis and hourly energy analysis conducted.

$$\text{RTU cooling energy use (Wh/day)} = 45.7168 + 2.5068 * (T_i - 7.0872)^+ + 0.0028 * S_i \quad (5)$$
$$(R^2 = 0.97)\,.$$

$$\text{VAV reheat energy use (Wh/day)} = 144.9539 - 10.7478 * (T_i - 14.3503)^- - 124 * (T_i - 20.1672)^+ - 0.0309 * S_i \quad (6)$$
$$(R^2 = 0.80)\,.$$

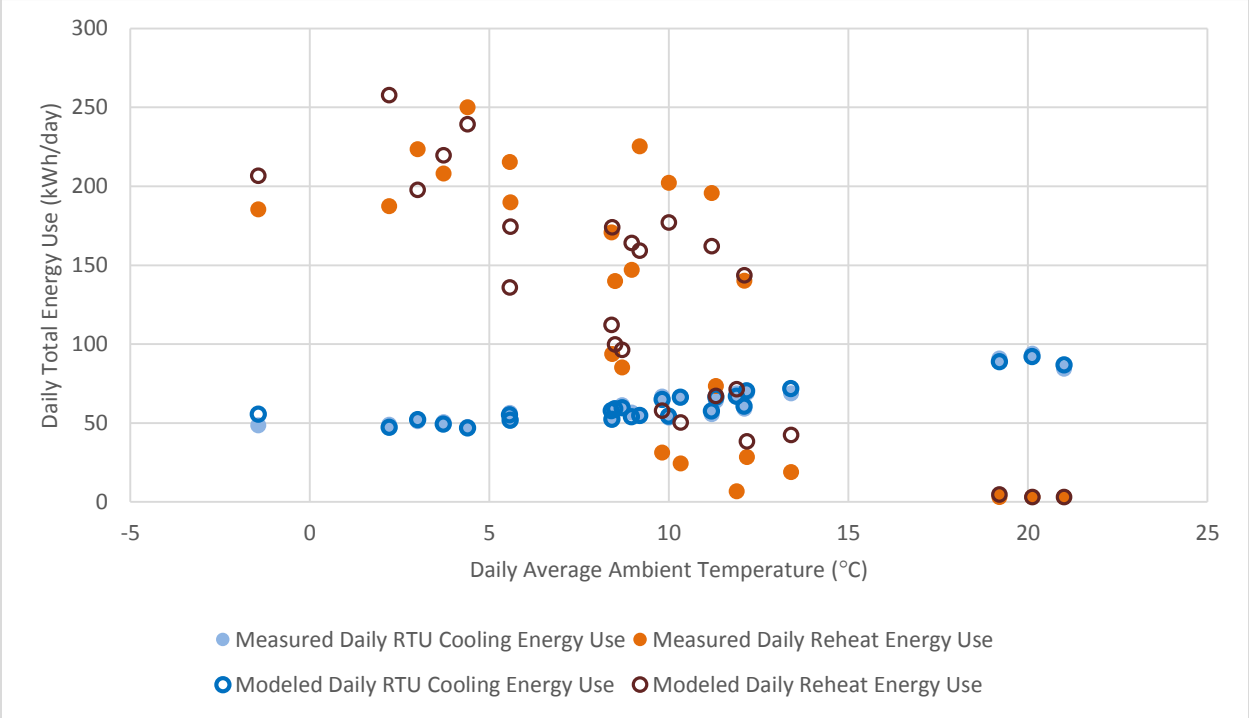

Fig. 25. Daily RTU cooling and reheat energy use (measured vs. modeled).

6.1.2 VRF–Thermostat Daily Energy Use

Fig. 26 shows a scatter-plot of daily total VRF energy use versus daily average OA temperature when the system was controlled by thermostat settings. Since the installed VRF system is a heat pump type of system, which cannot provide simultaneous cooling and heating to different zones, the operating mode was controlled by a master thermostat installed in room 105. An IMT-generated 5-parameter model with daily average OA temperature (T_i) and daily total global solar radiation (S_i, W/m^2) shown in Eq. (7) fits well with the measured data. Apparently, the change-point temperatures for heating and cooling were around 7° and 18°C, respectively. In other words, during days with an average OA temperature below 7°C, heating was the dominant energy use. During days with an average OA temperature above 18°C, cooling was the dominant energy use. During days with OA temperatures between 7 and 18°C, there were small heating and cooling needs, a minimum of about 30 kWh per day.

$$\text{VRF energy use } \left(\frac{\text{Wh}}{\text{day}}\right) = 39.6987 - 7.9398 * (T_i - 6.9010)^- + 12.1715 * (T_i - 17.7810)^+ - 0.0029 * S_i \ (R^2 = 0.96). \quad (7)$$

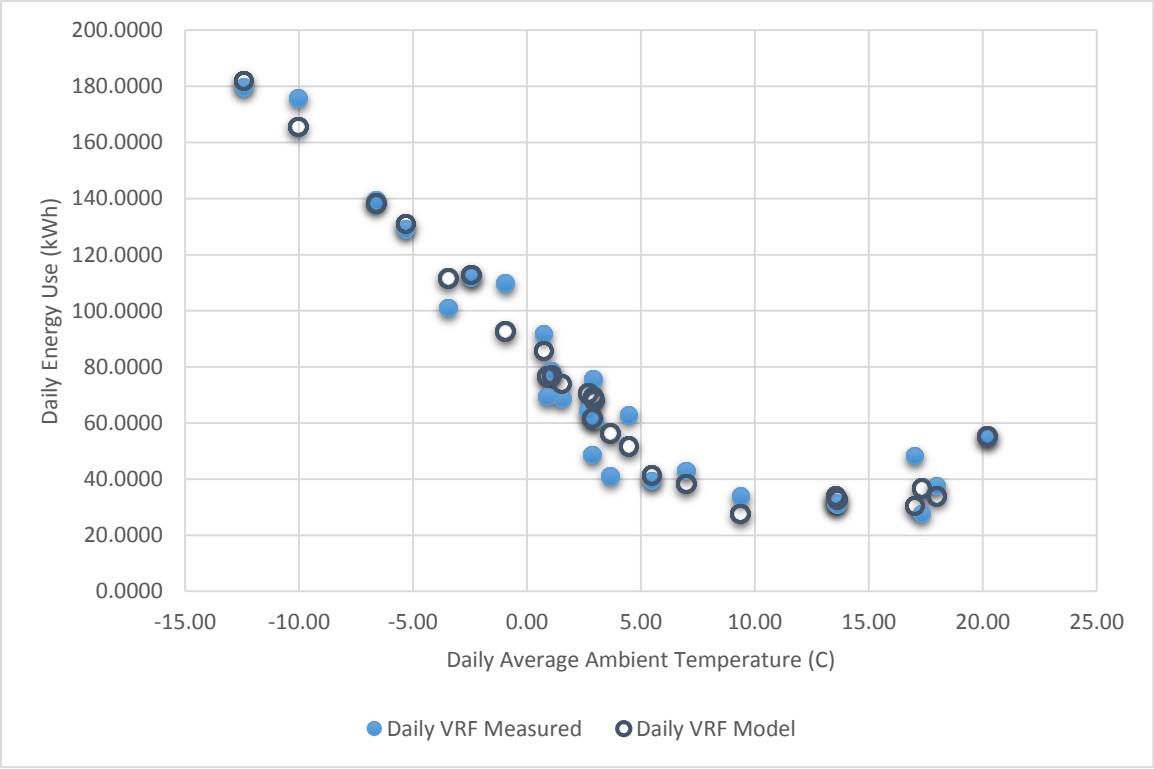

Fig. 26. Daily energy use for VRF–thermostat (measured vs. modeled).

6.1.3 VRF–CCM Daily Energy Use

Fig. 27 shows a scatter-plot of daily total VRF energy use versus OA temperature when the system is controlled by the CCM control algorithm. Similar to VRF–thermostat, the operation mode was controlled by a master thermostat installed in room 105. The energy use profile for the VRF–CCM in Fig. 27 is similar to that for the VRF–thermostat scenario for the higher OA temperature range. An IMT 5-parameter model with daily average OA temperature (T_i) and daily total global solar radiation (S_i, W/m^2) shown in Eq. (8) fit well with the measured data. One of the distinct differences between thermostatic control and CCM control was the energy use during mild outdoor conditions. Apparently, the change-point temperatures for heating and cooling were around 9 and 18°C, respectively. In other words, during days with average OA temperatures below 9°C, heating was the dominant energy use. During days with average OA temperatures above 18°C, cooling was the dominant energy use. During days with OA temperatures between 9 and 18°C, there were small heating and cooling needs—a minimum of about 10 kWh per day, which is about 10 kWh less than in the VRF–thermostat scenario. This was partially due to the existence of a larger dead band in the CCM control scenario than in thermostatic control; it was also partially due to continuous indoor fan operation in thermostatic control versus intermittent fan operation in CCM control (i.e., there was more fan power consumption in thermostatic control).

$$\mathrm{VRF_{CCM}\,energy\ use}\left(\frac{\mathrm{Wh}}{\mathrm{day}}\right) = 30.544 - 5.8051 * (\mathrm{T_i} - 8.848)^{-} + 11.3463 * (\mathrm{T_i} - 17.672)^{+} - 0.0049 * \mathrm{S_i}\ (R^2 = 0.79)\ . \quad (8)$$

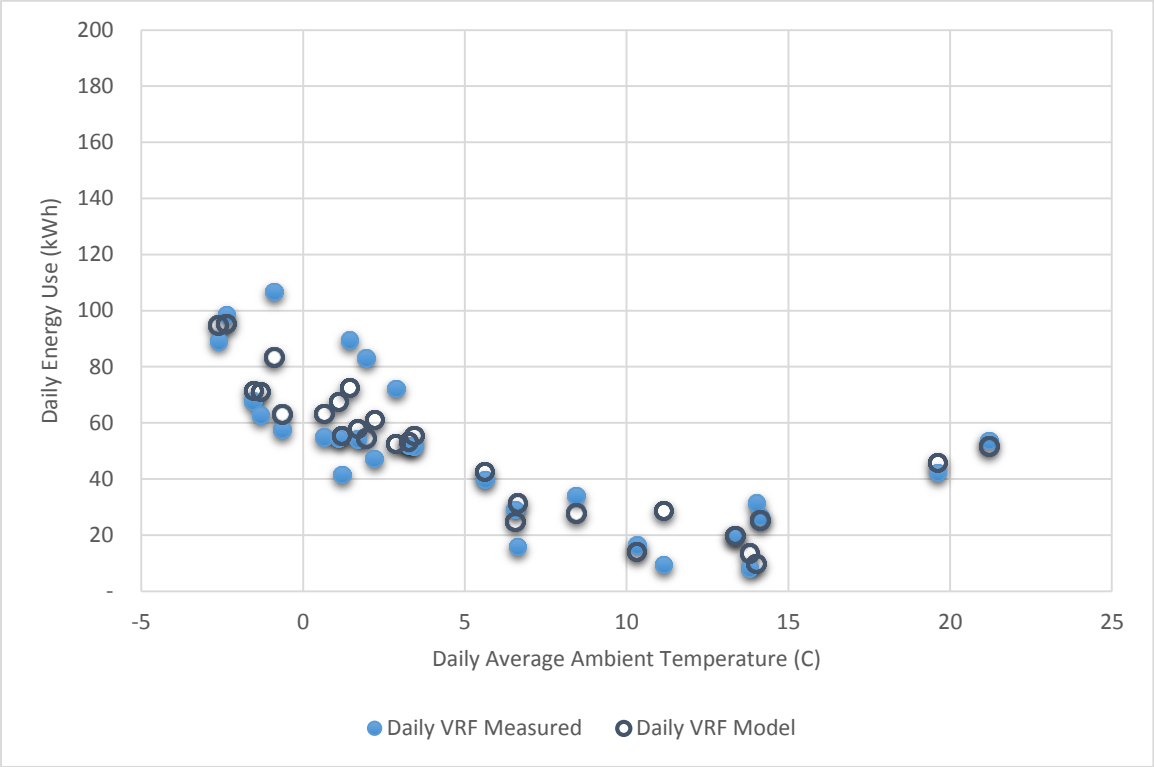

Fig. 27. Daily energy use for VRF–CCM control (measured vs. modeled).

6.1.4 Energy Use Comparison

Based on the inverse models—with the daily average OA temperature and the daily total global solar radiation as independent variables—the daily energy use for the RTU, VRF–thermostat, and VRF–CCM scenarios from October 1, 2014, through February 28, 2015, was estimated (as shown in Fig. 28).

Table 10 and Fig. 29 show the aggregated monthly energy use data for the three systems/controls, which show that the VRF–thermostat scenario used 74% less energy than the RTU scenario, and the VRF–CCM used 80% less energy than RTU. Compared with VRF–thermostat, VRF-CCM used 23% less energy.

Although the comparison revealed that the RTU system was using significantly more energy than the VRF system in heating season, there are several limitations to this analysis:

1. The RTU system was using electric reheat. If hot water reheat with an 80% AFUE gas boiler were used, the source energy savings would be only about 53% for the VRF system with thermostat control.
2. The discharge air temperature for the RTU system was fixed to 14°C even during the heating season, which resulted in excessive reheat energy use. If the discharge air temperature were based on an OA reset schedule, RTU direct exchange cooling and reheat energy use would be reduced significantly.

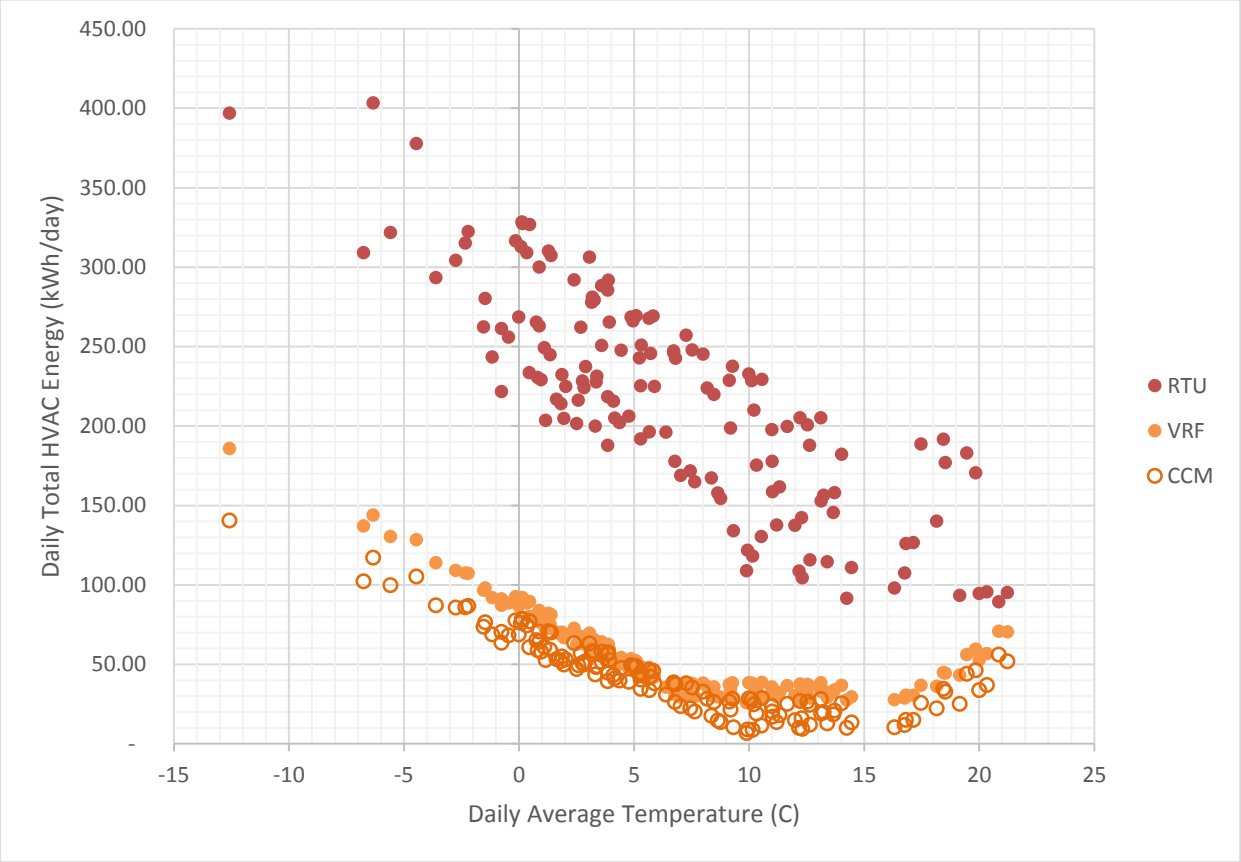

Fig. 28. Modeled daily energy use for RTU, VRF–thermostat, and VRF–CCM.

Table 10. Monthly RTU, VRF, and CCM energy use

Year	Month	Average of OA (C)	Average daily solar radiation (Wh/m²)	RTU (kWh)	VRF (kWh)	CCM (kWh)
2014	10	15.0	3,164.2	4,141.9	1,168.5	696.8
2014	11	5.7	2,453.3	6,547.9	1,562.3	1,220.4
2014	12	6.6	1,438.8	7,365.6	1,566.6	1,283.4
2015	1	3.9	2,179.6	5,822.8	1,458.4	1,185.4
2015	2	0.2	2,687.3	7,225.9	2,351.5	1,841.2
Grand total				**31,104**	**8,107**	**6,227**
% difference from RTU					**74%**	**80%**
% difference from VRF–thermostat						**23%**

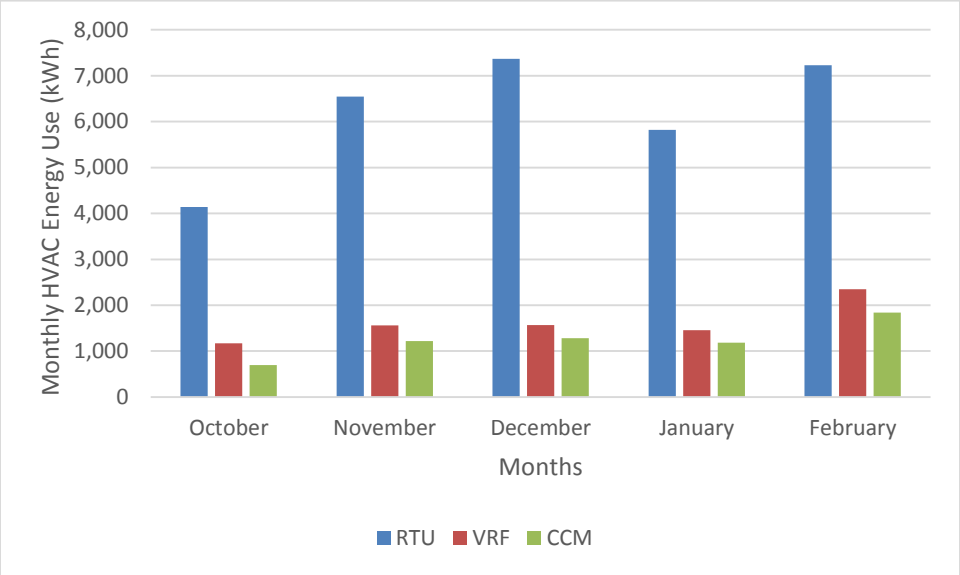

Fig. 29. Monthly daily energy use for RTU, VRF–thermostat, and VRF–CCM.

6.2 Thermal Comfort Analysis

Thermal comfort for each of the ten thermal zones was analyzed for each scenario, using the measured hourly indoor temperature and PMV/PPD metrics.

6.2.1 Indoor Temperature

Fig. 30 presents the indoor temperature statistics for RTU, VRF-thermostat, and VRF-CCM.

- The median zone temperatures for RTU operation show that the zones downstairs were slightly underheated.
- The median zone temperatures for VRF–thermostat show that the zone temperatures were relatively well maintained. Higher variations in the indoor temperatures for rooms 105,106, 205, and 206 were possibly due to the solar heat gains through the windows during the afternoons. Since the system cannot provide simultaneous heating and cooling, some zones (e.g., rooms 205 and 206) showed a maximum temperature approaching 27°C, which could cause uncomfortable thermal conditions.
- For VRF–CCM, the median zone temperatures were similar to those for VRF–thermostat. However, the variation in the zone temperatures was higher, as was expected because of the larger dead band in the CCM control.

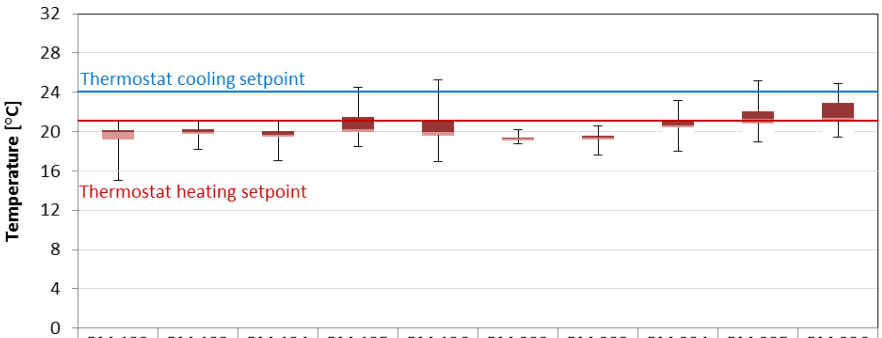

	RM 102	RM 103	RM 104	RM 105	RM 106	RM 202	RM 203	RM 204	RM 205	RM 206
Max	21.1	21.1	21.1	24.5	25.3	20.2	20.6	23.2	25.2	24.9
Q3	20.2	20.2	20.0	21.5	21.1	19.4	19.6	21.1	22.1	22.9
Median	19.9	20.0	19.7	20.3	20.0	19.3	19.4	20.7	21.3	21.4
Q1	19.2	19.8	19.5	19.9	19.6	19.1	19.2	20.4	20.9	21.0
Min	15.0	18.2	17.1	18.5	17.0	18.8	17.6	18.0	18.9	19.4

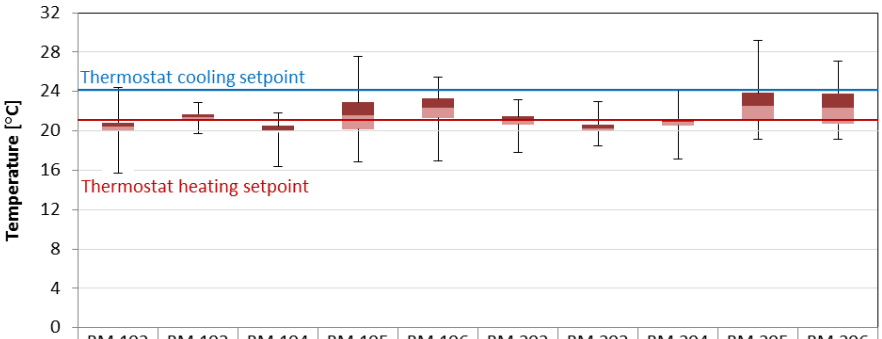

	RM 102	RM 103	RM 104	RM 105	RM 106	RM 202	RM 203	RM 204	RM 205	RM 206
Max	24.4	22.8	21.8	27.6	25.5	23.2	23.0	24.3	29.2	27.1
Q3	20.9	21.7	20.5	22.9	23.3	21.5	20.7	21.2	23.8	23.8
Median	20.5	21.4	20.1	21.6	22.4	21.0	20.3	20.9	22.5	22.4
Q1	20.0	21.1	19.9	20.2	21.3	20.7	20.0	20.6	21.2	20.7
Min	15.7	19.7	16.4	16.8	16.9	17.8	18.5	17.2	19.1	19.2

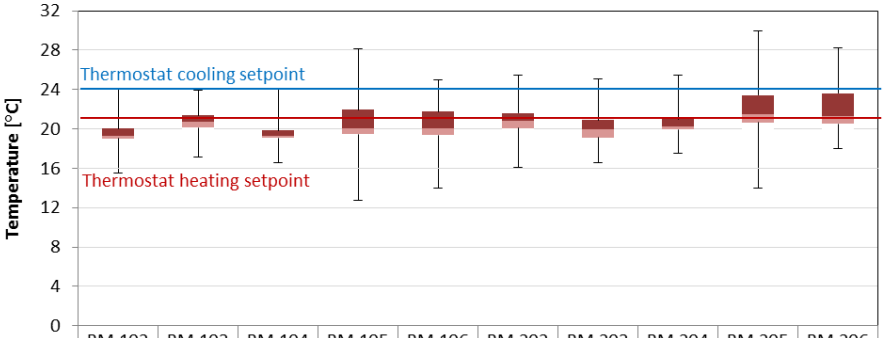

	RM 102	RM 103	RM 104	RM 105	RM 106	RM 202	RM 203	RM 204	RM 205	RM 206
Max	24.1	24.0	24.0	28.1	25.0	25.5	25.0	25.5	29.9	28.2
Q3	20.0	21.4	19.9	22.0	21.8	21.6	20.9	21.0	23.5	23.6
Median	19.3	20.8	19.3	20.0	20.0	20.8	20.0	20.2	21.5	21.3
Q1	19.0	20.1	19.1	19.4	19.4	20.1	19.1	19.9	20.7	20.5
Min	15.5	17.1	16.5	12.7	13.9	16.1	16.6	17.5	13.9	18.0

Fig. 30. Heating season zone temperature by room for (a) RTU, (b) VRF-thermostat, and (c) VRF-CCM.

6.2.2 PMV/PPD Values

Further analysis of the indoor thermal conditions was performed using PMV metrics. PMV values for each of the ten zones were calculated and compared. The PMV range between −0.5 and 0.5 is considered acceptable for thermal comfort. PMV values greater than 0.5 indicate a warm/hot thermal sensation, whereas PMV values less than −0.5 indicate a cool/cold thermal sensation.

The hourly PMV values for each room for the three HVAC modes are shown in Fig. 31 through Fig. 33. The data show clearly that, for RTU, all rooms on the first and the second floor without southern exposure had all PMV values less than 0 (i.e., on the cooler side of the range), and most values were beyond −0.5. Rooms with southern exposure had PMV values greater than 0 for a few hours. However, they appear to have been as cool as the rooms that did not face south. VRF–thermostat and VRF–CCM had similar distributions of PMV values, except that the variation in the PMV values was wider for VRF–CCM.

The PMV statistics in Fig. 34 show the quantitative distribution of PMV values. For all three cases, room 102 shows the lowest minimum PMV, approaching −2.0. Room 102 has an exterior door without any buffer zone, which would have caused high OA infiltration that resulted in cold conditions. In all cases, most rooms (especially on the first floor) had PMV values exceeding −1, which indicates that the rooms were a little cool for some occupants. For VRF–CCM, the maximum PMVs of rooms 105, 205, and 206 exceeded 1, which indicates that the rooms could be too warm for some occupants. However, the data show that the higher PMVs occurred for only about 0.6% of the operating hours.
Table 11 shows the median PMV values for each room. Table 12 shows the percentage of hours during which PMV values were below −0.5 (a cool/cold sensation), between −0.5 and 0.5 (acceptable thermal comfort), and above 0.5 (a warm/hot sensation). As shown in Table 12, there were some thermal comfort issues (i.e., rooms that were too cold) during more than half of the operating hours for all three cases. Further investigation revealed three major reasons for the lower PMV values: (1) lower indoor temperature, (2) lower RH, and (3) an MRT about 1–2°C lower than the indoor temperature. All three conditions contributed to the lower PMV values. Since indoor temperature and humidity trends were found to be similar for all three systems, it is expected that better thermal comfort could be achieved if the thermostat settings for all three cases were increased by 1 or 2°C or if the RH in the rooms were increased by operating a humidifier.

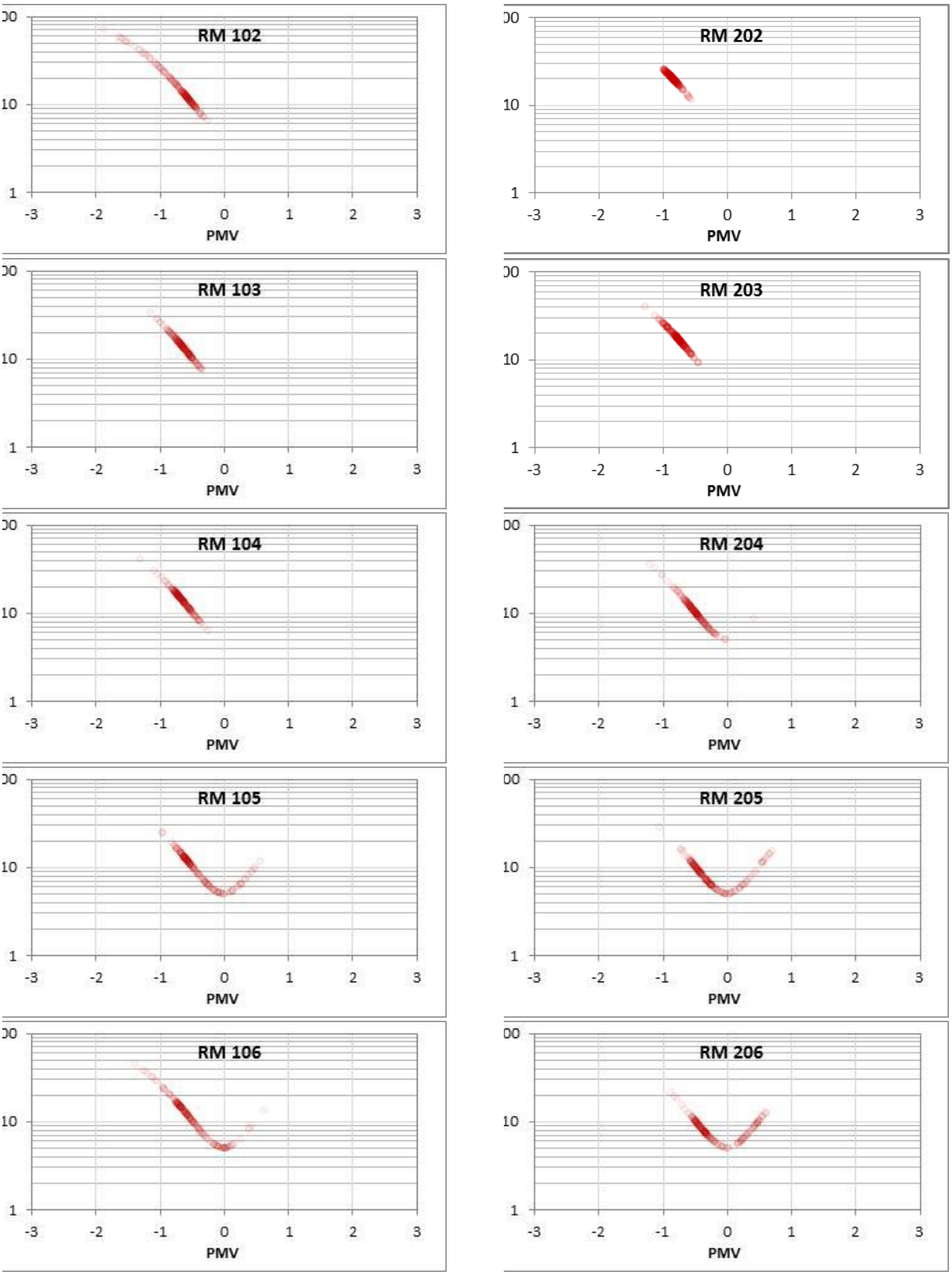

Fig. 31. Heating season PMV/PPD values by room for RTU.

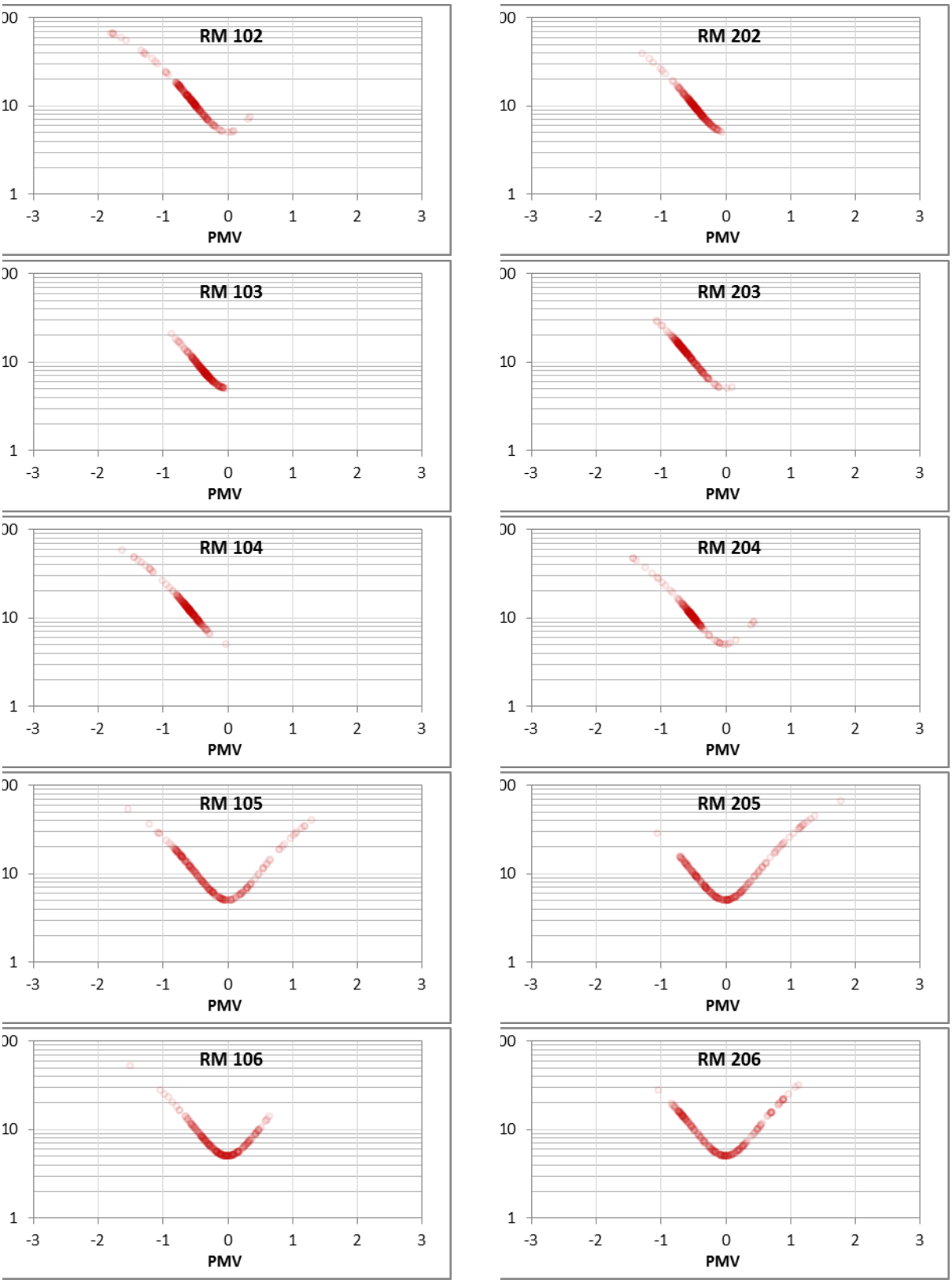

Fig. 32. Heating season PMV/PPD values by room for VRF–thermostat.

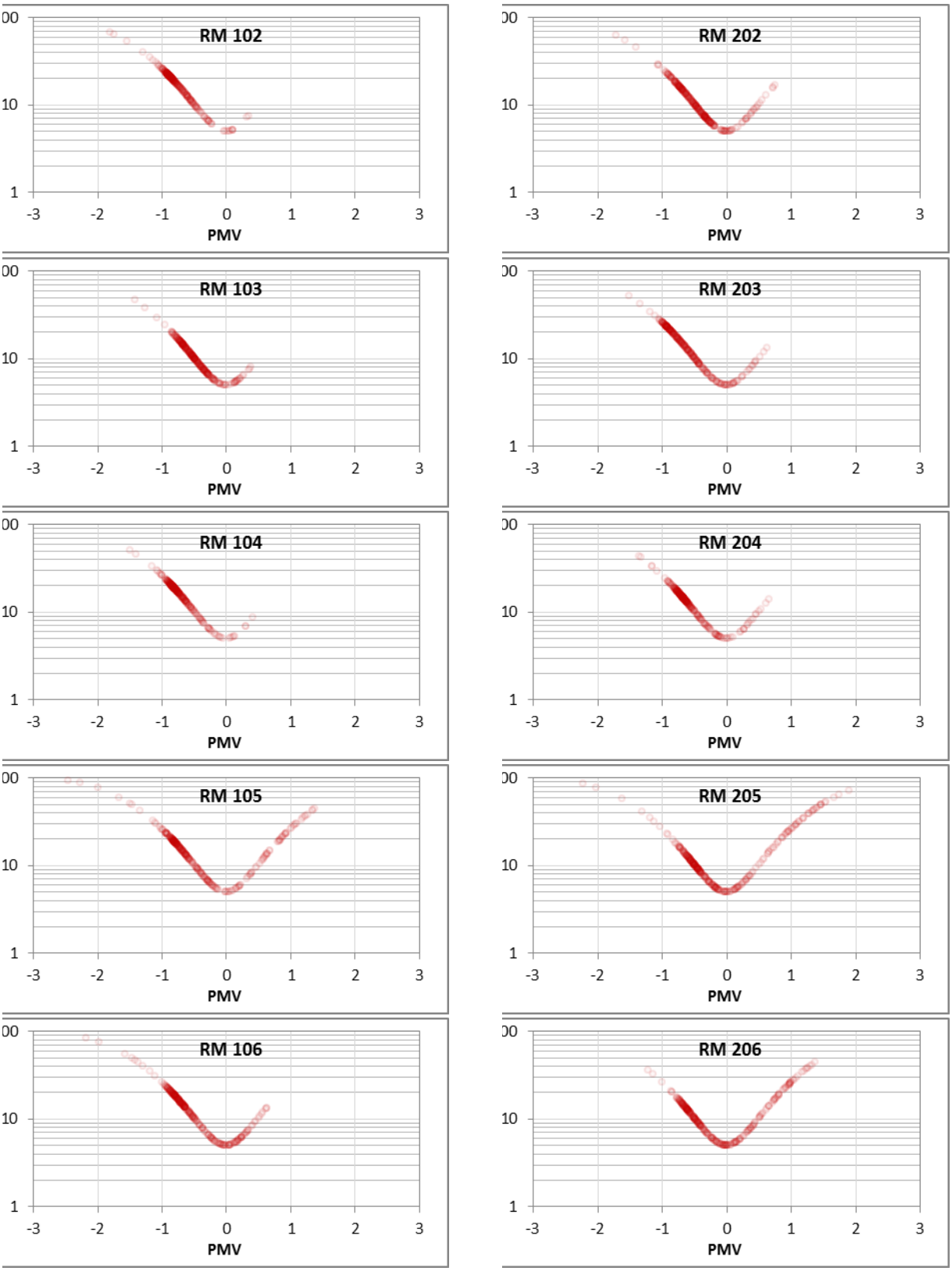

Fig. 33. Heating season PMV/PPD values by room for VRF–CCM.

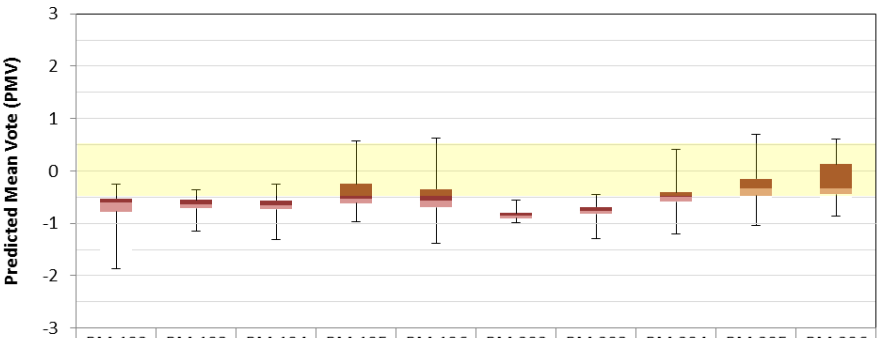

	RM 102	RM 103	RM 104	RM 105	RM 106	RM 202	RM 203	RM 204	RM 205	RM 206
Max	-0.26	-0.35	-0.25	0.57	0.63	-0.56	-0.45	0.42	0.70	0.60
Q3	-0.52	-0.55	-0.56	-0.24	-0.35	-0.80	-0.69	-0.41	-0.15	0.12
Median	-0.60	-0.64	-0.66	-0.54	-0.57	-0.85	-0.76	-0.49	-0.33	-0.33
Q1	-0.77	-0.71	-0.73	-0.61	-0.70	-0.90	-0.82	-0.59	-0.47	-0.44
Min	-1.87	-1.15	-1.31	-0.97	-1.39	-0.99	-1.29	-1.21	-1.04	-0.87

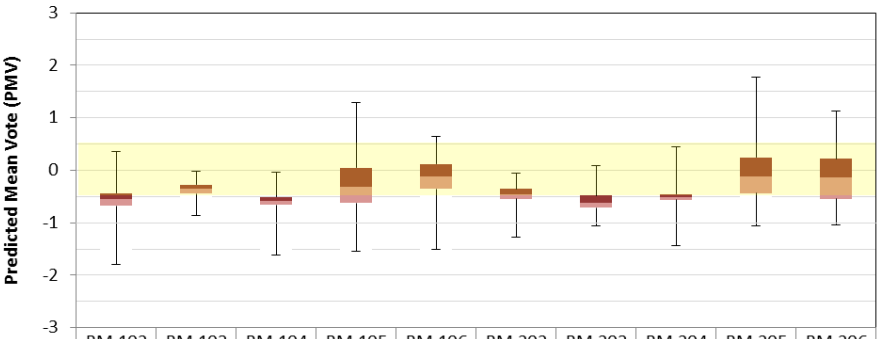

	RM 102	RM 103	RM 104	RM 105	RM 106	RM 202	RM 203	RM 204	RM 205	RM 206
Max	0.35	-0.02	-0.03	1.29	0.65	-0.06	0.09	0.44	1.77	1.13
Q3	-0.44	-0.27	-0.51	0.05	0.12	-0.35	-0.48	-0.46	0.24	0.22
Median	-0.54	-0.35	-0.59	-0.32	-0.11	-0.46	-0.61	-0.52	-0.12	-0.14
Q1	-0.68	-0.44	-0.66	-0.62	-0.36	-0.54	-0.71	-0.56	-0.43	-0.54
Min	-1.79	-0.87	-1.62	-1.54	-1.51	-1.28	-1.06	-1.43	-1.05	-1.04

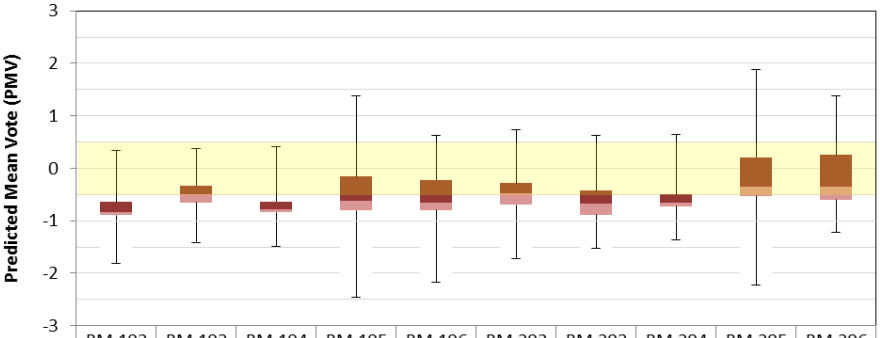

	RM 102	RM 103	RM 104	RM 105	RM 106	RM 202	RM 203	RM 204	RM 205	RM 206
Max	0.34	0.38	0.42	1.37	0.63	0.74	0.63	0.65	1.89	1.37
Q3	-0.64	-0.33	-0.64	-0.16	-0.22	-0.28	-0.42	-0.50	0.21	0.25
Median	-0.84	-0.50	-0.79	-0.63	-0.65	-0.48	-0.68	-0.66	-0.36	-0.35
Q1	-0.90	-0.65	-0.84	-0.80	-0.79	-0.70	-0.88	-0.72	-0.53	-0.60
Min	-1.81	-1.43	-1.49	-2.46	-2.17	-1.71	-1.52	-1.36	-2.23	-1.22

Fig. 34. Heating season PMV statistics by room for (a) RTU, (b) VRF–thermostat, and (c) VRF–CCM.

Table 11. Median PMV values by room for RTU, VRF–thermostat and VRF–CCM

	RM 102	RM 103	RM 104	RM 105	RM 106	RM 202	RM 203	RM 204	RM 205	RM 206
RTU	−0.60	−0.64	−0.66	−0.54	−0.57	−0.85	−0.76	−0.49	–0.33	–0.33
VRF–thermostat	−0.54	−0.35	−0.59	−0.32	−0.11	−0.46	−0.61	−0.52	–0.12	–0.14
VRF–CCM	−0.84	−0.50	−0.79	−0.63	−0.65	−0.48	−0.68	−0.66	–0.36	–0.35

Table 12. Percentage of operating hours meeting thermal comfort criteria

	PMV below –0.5 (Colder)	PMV between –0.5 and 0.5 (Comfort)	PMV above 0.5 (Warmer)
RTU	65.0%	33.9%	1.1%
VRF–thermostat	41.8%	54.0%	4.2%
VRF–CCM	60.3%	33.8%	5.9%

6.3 Performance during a Typical Winter Day

Fig. 35 shows the hourly RTU and VRF–thermostat energy consumption and room temperatures for a typical winter day.

- In general, both systems show similar patterns for energy use. Both systems show high energy use at system startup 6:00 a.m. to reach the new set point temperature (i.e., 21°C) quickly as the occupancy mode changes from “unoccupied” to “occupied.” The energy use decreases as the room temperature reaches the set point temperature. However, the RTU used more energy (about twice as much as the VRF) during system startup.
- After the morning startup, the RTU system slightly overheated the space and then allowed the temperature to drop gradually. On the other hand, the VRF system cycled to maintain the room temperature in a narrow range.
- During late afternoons in the winter, the south-facing rooms (particularly rooms 205 and 206) show higher zone temperatures during VRF system operation. On the other hand, the RTU system maintained the temperature in these rooms within a narrow range according to the thermostat settings. This is because the VRF system cannot provide simultaneous heating and cooling to the building and rooms 205 and 206 with high solar heat gains could not be cooled down.

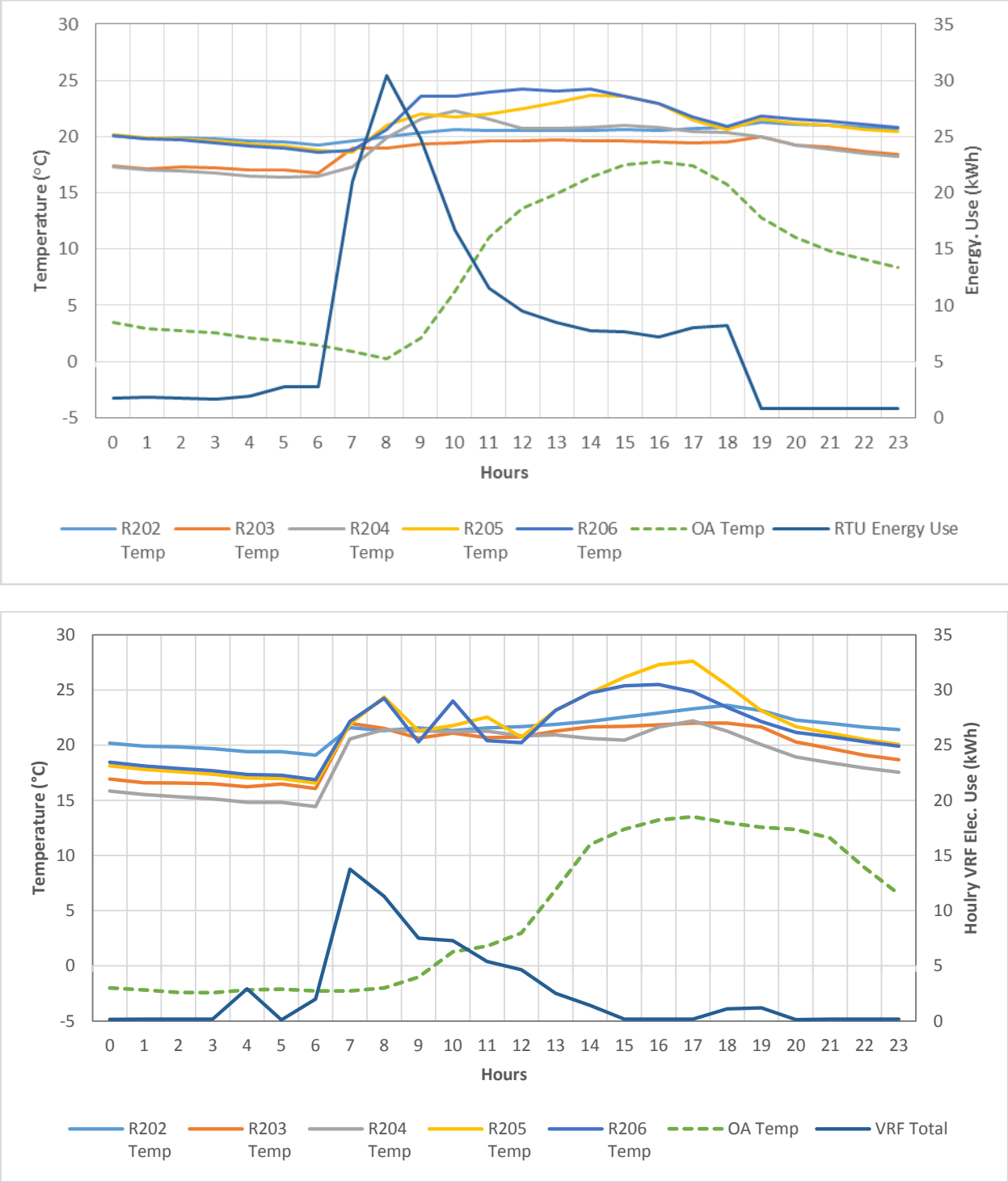

Fig. 35. Hourly energy consumption and room temperatures for a typical winter day for (a) RTU and (b) VRF system.

7. ANNUAL ENERGY ANALYSIS USING ENERGYPLUS SIMULATION

This study used both field measurement data and an hourly building energy model to analyze the energy performance of the RTU and VRF systems. The energy modeling was particularly useful in this project for evaluating the annual energy performance of the systems, because the FRP was operated with each system alternately and a complete full year of data was not available from any of the systems. In addition, the energy modeling allowed performance comparison of the VRF system and the alternative baseline system.

For the energy modeling, DOE's flagship building energy modeling software, EnergyPlus 8.1, was used. EnergyPlus 8.1 currently provides VRF system modeling capability as well as modeling of single-package RTUs with VAV reheat. The baseline and the VRF system models were developed using EnergyPlus (Fig. 36), and the model was calibrated by comparing the hourly measured data until they reasonably matched based on the definition from ASHRAE Guideline 14P (ASHRAE 2002).[6] Using the calibrated model with actual weather files, full-year energy performance was analyzed for each system.

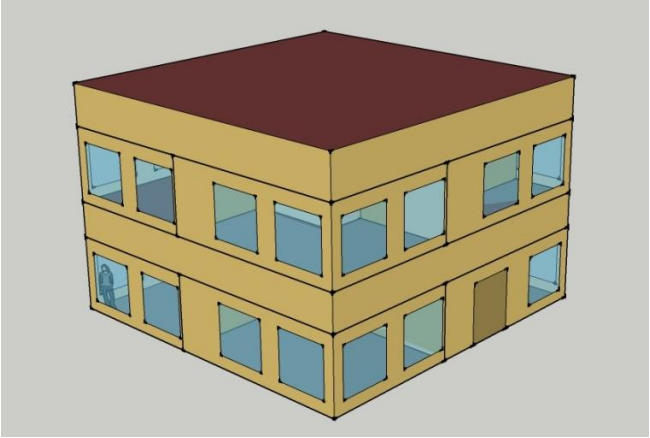

Fig. 36. Three-dimensional rendering of the EnergyPlus model of the two-story FRP.

7.1 EnergyPlus Model

An initial EnergyPlus model for the two-story FRP with VRF systems was developed based on the architectural/mechanical drawings, manufacturer specification, and site audit. An attempt has not yet been made to fully calibrate the initial model with the measured data, but the energy use results for the partially calibrated model nonetheless show a close match with the measured data, as shown in Fig. 37.

[6] The first year study pursues a partially calibrated energy model. The model will be further refined in year 2.

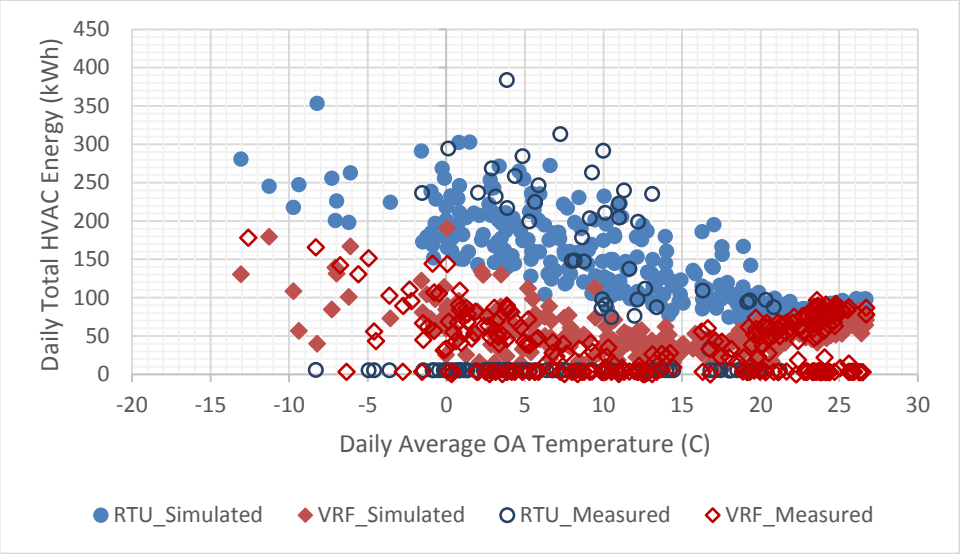

Fig. 37. Measured versus simulated daily RTU and VRF energy use.

7.2 As-Is Annual Energy Savings (RTU vs. VRF)

To estimate the annual energy savings using the calibrated models, the actual weather file for 2014 was used; it was generated using the data from the weather station at the FRP. Fig. 38 shows the annual end-use energy savings. It shows that the VRF systems would result in 60% HVAC energy use savings and 38% whole-building energy use savings compared with the RTU system. These savings include 71% for heating, 22% for cooling, and 78% for fan energy use. The saving estimates are comparable to the estimates made in Section 6. As expected, the highest savings (i.e., 21,415 kWh) would be for heating energy, as the RTU uses electric resistance reheat.

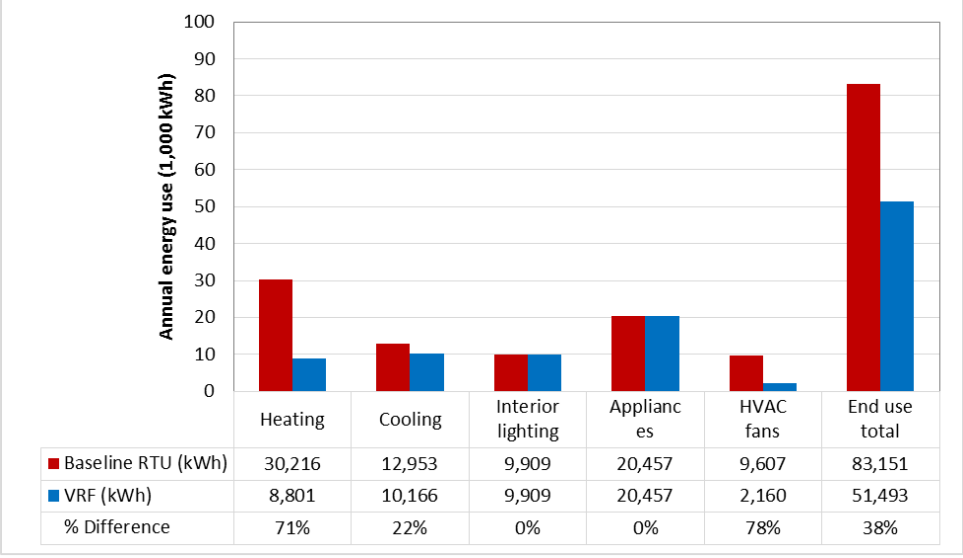

	Heating	Cooling	Interior lighting	Appliances	HVAC fans	End use total
Baseline RTU (kWh)	30,216	12,953	9,909	20,457	9,607	83,151
VRF (kWh)	8,801	10,166	9,909	20,457	2,160	51,493
% Difference	71%	22%	0%	0%	78%	38%

Fig. 38. Simulated RTU and VRF annual energy end uses.

7.3 Annual Energy Savings for Alternative RTU Baseline Systems

7.3.1 RTU System with Discharge Air Temperature Reset

The current RTU system is programmed to deliver the discharge air at a constant temperature of 14ºC. This is likely to cause excessive electric reheat energy use during the heating season. The energy saving potential of the VRF system compared with this alternative RTU system was estimated, using the calibrated simulation model, by modifying the RTU system to have a reset schedule. The reset schedule was specified to provide discharge air at 14°C from April through September and at 16°C for the rest of the year. The simulation results in Table 13 show that with the discharge air temperature reset, the RTU cooling and heating energy use would decrease by about 706 kWh (6%) and 5,280kWh (18%), respectively. The VRF system would result in 55% HVAC energy savings and 33% whole-building energy savings compared with the alternative RTU system.

Table 13. Simulated annual energy use for the RTU with discharge air temperature reset versus the VRF system

End use	RTU (kWh)	VRF (kWh)	Difference (kWh)	Difference (%)
Heating	24,936	8,801	16,135	65
Cooling	12,247	10,166	2,081	17
Interior lighting	9,909	9,909	–	0
Interior equipment	20,457	20,457	–	0
HVAC fans	9,609	2,160	7,449	78
Total end uses	77,158	51,493	31,657	33

7.3.2 RTU System with Hot Water Reheat and Discharge Air Temperature Reset

The current baseline RTU system uses electric reheat to provide heating to the zones. If hot water reheat provided by an 80% AFUE natural gas boiler were considered, additional source energy savings would result. Table 144 shows the simulated energy use of the RTU system with hot water reheat versus the VRF system. Using source energy factors for the delivered electricity and delivered natural gas from Deru and Tocellini (2007),[7] source energy use for the two systems was determined. It shows that the VRF system would result in 124,700 MBtu (33%) HVAC-related source energy savings (i.e., 17% source energy savings if whole-building energy use is considered) compared with the RTU system with hot water reheat.

[7] The source energy factors for electricity and the natural gas are 3.443 and 1.092, respectively, for the US Eastern Interconnection.

Table 14. Simulated annual energy use for RTU with hot water reheat versus VRF system

End use	Site energy			Source energy			
	RTU w/HW reheat		VRF	RTU w/HW reheat		VRF	Difference (%)
	Electricity (kWh)	Natural gas (MBtu)	Electricity (kWh)	Electricity (MBtu)	Natural gas (MBtu)	Electricity (MBtu)	
Heating	–	106,352	8,801	-	116,136	103,390	11
Cooling	12,247	–	10,166	143,872	–	119,425	17
Lighting	9,909	–	9,909	116,406	–	116,406	0
Interior eqpt.	20,457	–	20,457	240,319	–	240,319	0
HVAC fans	9,609	–	2,160	112,882	–	25,375	78
End use total	52,222	106,352	51,493	613,479	116,136	604,915	17

7.3.3 Summary of Comparison of VRF System with Alternative RTU Baseline System

Table 15 summarizes the site and source energy savings, energy cost savings, and resulting CO_2 emission reductions from the VRF system compared with the alternative RTU baseline systems. Using the US average electricity and natural gas rates in 2014 (i.e., \$0.1062/kWh for electricity and \$8.9/Mcf [1,000 ft^3] for natural gas), the annual energy cost for each system was calculated. Using the CO_2 emission factors for the delivered electricity and natural gas from Deru and Tocellini (2007) (i.e., the emission factor of 1.64 lb per kWh of delivered electricity, the site burning emission factor of 122 lb per MMBtu of natural gas, and the pre-combustion emission factor of 11.6 lb per MMBtu of natural gas), the reduction in CO_2 emissions was calculated. The results show that the VRF system would result in 33 to 60% savings in HVAC-related source energy compared with the baseline RTUs. The corresponding annual energy cost savings would be around \$1,000 to \$3,300. The project energy savings would result in about 7 to 26 ton (~13 to 52 lb) of CO_2 emission reductions.

Table 15. Energy use, operating cost, and CO_2 emission reductions from VRF system

	VRF	Baseline 1 RTU as-is	Baseline 2 RTU with discharge reset	Baseline 3 RTU with discharge reset and hot water reheat
HVAC-related site energy use (MBtu)	72,085	180,072	159,654	180,925
Percent difference VRF vs. baseline		60%	55%	60%
HVAC-related source energy use (MBtu)	248,190	619,987	549,690	372,890
Percent difference VRF vs. baseline		60%	55%	33%
Annual energy cost (\$)	\$ 2,244	\$ 5,605	\$ 4,969	\$ 3,242
Energy cost savings (\$)		\$ 3,361	\$ 2,726	\$ 998
Percent difference VRF vs. baseline		60%	55%	31%
CO_2 emissions (lb)	34,648	86,553	76,739	47,755
CO_2 emission reductions (lb)		51,904	42,091	13,107
Percent difference VRF vs. baseline		60%	55%	27%

8. CONCLUSION AND LESSONS LEARNED

8.1 Summary and Conclusions

In this study, the performance of a Samsung VRF system was investigated by comparing it with a baseline rooftop VAV system. In addition, an enhanced control algorithm, CCM (comfort control method), was applied to the VRF system to evaluate further energy savings potential. The investigation was based on the analysis of the measured data from an occupancy-emulated small office building, the FRP, from July 2014 through February 2015. Calibrated simulation models were also used to estimate the annual energy performance of the baseline and VRF system. The following are the key findings and lessons learned from this case study.

Cooling Season Performance

- Cooling season data were monitored from July 7 through September 30, 2014. The energy consumption for the RTU and the VRF shows lower VRF energy use at moderate OA temperatures, with a diminishing difference as the OA temperature approached 30°C. This finding was expected because of the better part-load performance of VRF systems compared with the RTU. In addition, the RTU system shows increasing energy use below 15°C due to the VAV reheat energy use.

- During occupied periods, the VRF–thermostat and VRF–CCM used 11% and 19% less energy, respectively, than the RTU. The VRF–CCM used about 9% less energy than the VRF–thermostat. Accounting for the unoccupied periods, the VRF–thermostat and VRF–CCM saved about 17% and 26% in energy use, respectively, compared with the RTU. The VRF–CCM used about 10% less energy than the VRF–thermostat.

- The cooling season indoor thermal comfort analysis shows that VRF–thermostat provided similar or better thermal comfort compared with the RTU system. The median zone temperature for RTU operation shows that some rooms were slightly overcooled, particularly on the first floor. In VRF–CCM mode, several rooms were close to a 30°C maximum zone temperature, which could be uncomfortable for most occupants. Further algorithm updates will be considered to improve thermal comfort for the zones, especially for the perimeter zones.

Heating Season Performance

- Heating season data were monitored from October 1, 2014, through February 28, 2015. The weather-normalized energy use data for the RTU, VRF–thermostat, and VRF–CCM systems show that VRF–thermostat mode used 74% less energy than RTU, and VRF–CCM mode used 80% less energy than RTU. Compared with VRF–thermostat, VRF–CCM showed 23% less energy use.

- The heating season indoor thermal comfort analysis shows that the RTU and VRF–thermostat modes provided similar levels of thermal comfort. The median zone temperature for RTU shows that the zones were slightly underheated, particularly those on the first floor. It appears that the sun-facing

perimeter zones required cooling and other zones required heating, but the heat pump–type VRF system could not provide simultaneous cooling and heating. Therefore, there is a potential for uncomfortable thermal conditions. A heat recovery–type VRF system might resolve the issue. For VRF–CCM, the median zone temperatures were similar to those of VRF–thermostat. However, the variation in the zone temperatures was higher, which was expected because of the larger dead band in the CCM control.

Annual Energy Use

- An EnergyPlus building energy model was developed and simulated with the baseline RTU system and the VRF system. The model was calibrated using the hourly energy data and used to evaluate the annual energy performance of both systems. The calibrated model, simulated with the 2014 actual weather data for Oak Ridge, Tennessee, estimated that the VRF system would use about 60% less energy (i.e., 31,649 kWh/year less) than the RTU system. This included 71% (21.415 kWh/year) heating energy savings, 22% (2,787 kWh/year) cooling energy savings, and 78% (i.e., 7,448 kWh/year) fan energy savings.

- When an OA rest schedule was applied to the RTU discharge air temperature in the calibrated model, the RTU cooling and heating energy use decreased by about 706 kWh (6%) and 5,280 kWh (18%), respectively. As a result, the HVAC energy savings estimated from the VRF system would be 55% compared with the RTU.

8.2 Future Work

This study confirms the potential of a VRF system to reduce energy use and enhance indoor thermal comfort. At the same time, it emphasizes the need to explore several other aspects of the performance of the VRF systems. The following are some potential future efforts to pursue to better understand the behavior of the VRF system and improve its performance.

- **Analysis of part-load performance of VRF system:** VRF systems are well known for their superior part-load performance compared with conventional HVAC systems. A potential future study would be to evaluate the part-load performance of a VRF system in a real building (such as the FRP) and compare the study data with the manufacturer's performance data and data for other conventional systems.
- **Analysis of VRF system performance in different climates:** To evaluate the performance of a VRF system in different climates, energy simulation–based analysis would be the preferred and most cost-effective approach. A building energy model could be developed, calibrated using the measured VRF system performance data, modified according to building energy codes for selected climates, and simulated with corresponding typical meteorological year weather files.
- **Performance comparison of VRF system with different baseline systems:** This study compared the performance of the VRF system only with the performance of an RTU, a relatively less efficient system. With so many alternative and high-efficiency systems commonly available and installed—such as air- and water-source heat pump systems and multi-stage HVAC—a comparison of the performance of a VRF system with those systems would be valuable.

- **Improvement of the CCM control:** Although the CCM control algorithm implemented on the VRF system in this study provided adequate thermal comfort most of the time in the cooling and heating seasons, there were times when it could not meet the needed heating and cooling loads in certain zones. Therefore, further enhancement of the CCM control algorithm is a potential future effort.
- **Evaluation of VRF system with CCM control in occupied buildings:** This study was conducted in the ORNL FRP, an unoccupied research building. Thermal comfort in the zones was analyzed using quantitative metrics such as indoor temperature and PMV/PPD indices. Since thermal comfort is a subjective sensation, the CCM algorithm must also be evaluated in occupied multi-zone buildings in the United States to confirm whether the majority of occupants are satisfied with CCM control.

REFERENCES

ASHRAE. 1989. ASHRAE/IES Standard 90.1-1989. Energy Efficient Design of New Buildings except Low-Rise Residential Buildings, American Society of Heating, Refrigeration and Air-Conditioning Engineers, Atlanta.

ASHRAE. 2013. ANSI/ASHRAE Standard 55-2013. Thermal Environmental Conditions for Human Occupancy, American Society of Heating, Refrigeration and Air-Conditioning Engineers, Atlanta.

ASHRAE. 2002. ASHRAE Guideline 14-2002. Measurement of Energy and Demand Savings, American Society of Heating, Refrigeration and Air-Conditioning Engineers, Atlanta.

Deru, M., and P. Tocellini. 2007. *Source Energy and Emission Factors for Energy Use in Buildings*, Technical Report, NREL/TP-550-38617, National Renewable Energy Laboratory.

Kissock, J. K., et al. 2003. Inverse Modeling Toolkit: Numerical Algorithms. KC-03-2-1 (RP-1050), *ASHRAE Transactions* 109, Part 2.

Rutkowski, H. 2008. *Whole Building Load Calculation (Manual N)*, 5th Edition, Air-Conditioning Contractors of America.

APPENDIX A. VRF FINAL DESIGN DOCUMENT

Refer to attachment A

Attachment A

SAMSUNG

Project Report

Two Story Flexible Research Platform

2014-01-06

1 Total Load Profile

1.1 Building1

Dept	Fl	Room	Area		Load per unit area		Required Capacity			Sum of capacity			Model	Qty	Nominal Capacity			Outdoor	Model	Nominal Capacity		Combi. Ratio	
			CAD	SALES	Cooling	Heating	Cooling		Heating	Cooling		Heating			Cooling		Heating			Cooling	Heating	Cooling	Heating
							TC	SHC	TC	TC	SHC	TC			TC	SHC	TC			TC	TC		
			sq.ft.	sq.ft.	BTU/h/sq.ft.	BTU/h/sq.ft.	BTU/h	BTU/h	BTU/h	BTU/h	BTU/h	BTU/h			BTU/h	BTU/h	BTU/h	-	-	BTU/h	BTU/h	%	%
Building1	2F									142500	102100	159000	AM007FNTDCH/AA	1	7500	5100	8500	CU-1	AM144FXVAFH/AA	144000	162000	99	98
													AM012FNTDCH/AA	1	12000	8000	13500						
													AM018FNTDCH/AA	1	18000	12200	20000						
													AM018FNNDCH/AA	2	18000	13600	20000						
	1F												AM007FNTDCH/AA	2	7500	5100	8500						
													AM018FNTDCH/AA	1	18000	12200	20000						
													AM018FNNDCH/AA	2	18000	13600	20000						

2 Piping & Wiring

2.1 CU-1

2.1.1 Detail Load Profile

1) Design condition: USA, Tennessee, Knoxville, Cooling 93.9/73.9, Heating 12.9/32.0

2) Load profile

Building			Unit		Liquid	Gas	H.P.Gas	Airflow	Nominal Capacity			Simulated Capacity			Combi. Ratio	
Dept	Fl	Room	Name	Model name					Cooling		Heating	Cooling		Heating	Cooling	Heating
									TC	SHC	TC	TC	SHC	TC		
-	-	-	-	-	in	in	in	CFM	BTU/h	BTU/h	BTU/h	BTU/h	BTU/h	BTU/h	%	%
Building1	1F		CU-1	AM144FXVAFH/AA	1/2"	1 1/8"		9535.32	144000		162000	138900		150100	98.96	98.14
	2F		AC-22	AM007FNTDCH/AA	1/4"	1/2"		240.14	7500	5100	8500	7300	5300	7900		
			AC-21	AM012FNTDCH/AA	1/4"	1/2"		293.12	12000	8000	13500	11700	7900	12800		
			AC-23	AM018FNTDCH/AA	1/4"	1/2"		370.81	18000	12200	20000	17600	12000	18900		
			AC-24	AM018FNNDCH/AA	1/4"	1/2"		388.47	18000	13600	20000	17500	13400	18900		
			AC-25	AM018FNNDCH/AA	1/4"	1/2"		388.47	18000	13600	20000	17500	13400	18900		
	1F		AC-11	AM007FNTDCH/AA	1/4"	1/2"		240.14	7500	5100	8500	7300	5300	7900		
			AC-12	AM007FNTDCH/AA	1/4"	1/2"		240.14	7500	5100	8500	7300	5300	7900		
			AC-13	AM018FNTDCH/AA	1/4"	1/2"		370.81	18000	12200	20000	17600	12000	18900		
			AC-14	AM018FNNDCH/AA	1/4"	1/2"		388.47	18000	13600	20000	17500	13400	18900		
			AC-15	AM018FNNDCH/AA	1/4"	1/2"		388.47	18000	13600	20000	17500	13400	18900		

2.1.2 Control

1) This data is for reference only. Verify local, state, and national electric codes. Samsung does not guarantee this data.

2) Configuration

Building			Unit		Transmission wires	Power wires	Breaker Fuse	Main Address		RMC Address		Accessories	
Dept	Fl	Room	Name	Model name								Optional accessories	Basic accessories
-	-	-	-	-	mm2	mm2	A						
Building1	1F		CU-1	AM144FXVAFH/AA	AWG~	AWG~	70						
	2F		AC-22	AM007FNTDCH/AA	AWG 18~16	AWG 16~14		0	6	0	0	MWR-WE10N	
			AC-21	AM012FNTDCH/AA	AWG 18~16	AWG 16~14		0	5	0	0	MWR-WE10N	
			AC-23	AM018FNTDCH/AA	AWG 18~16	AWG 16~14		0	7	0	0	MWR-WE10N	
			AC-24	AM018FNNDCH/AA	AWG 18~16	AWG 16~14		0	8	0	0	PC4SUSMEN,MWR-WE10N	
			AC-25	AM018FNNDCH/AA	AWG 18~16	AWG 16~14		0	9	0	0	PC4SUSMEN,MWR-WE10N	
	1F		AC-11	AM007FNTDCH/AA	AWG 18~16	AWG 16~14		0	0	0	0	MWR-WE10N	
			AC-12	AM007FNTDCH/AA	AWG 18~16	AWG 16~14		0	1	0	0	MWR-WE10N	
			AC-13	AM018FNTDCH/AA	AWG 18~16	AWG 16~14		0	2	0	0	MWR-WE10N	
			AC-14	AM018FNNDCH/AA	AWG 18~16	AWG 16~14		0	3	0	0	PC4SUSMEN,MWR-WE10N	
			AC-15	AM018FNNDCH/AA	AWG 18~16	AWG 16~14		0	4	0	0	PC4SUSMEN,MWR-WE10N	

2.1.3 Equipment list

1) Equipment list

Categories	Model name		Qty	Categories	Model name		Qty
DVM S(NEW)		AM144FXVAFH/AA	1	4 WAY CASSETTE (600x600) PANEL		PC4SUSMEN	4
NEO FORTE		AM007FNTDCH/AA	3	Distributor Kit		MEV-E24SA	4
		AM012FNTDCH/AA	1			MEV-E32SA	2
		AM018FNTDCH/AA	2	Y-Joint		MXJ-YA2812M	1
4 WAY CASSETTE (600x600)		AM018FNNDCH/AA	4			MXJ-YA2512M	3
WIRED REMOTE CONTROLLER		MWR-WE10N	10			MXJ-YA1509M	5

2) Piping length

Length as pipe diameter		1/4"	3/8"	1/2"	5/8"	3/4"	7/8"	1"	1 1/8"	1 1/4"	1 3/8"	1 1/2"	1 5/8"	1 3/4"	1 7/8"	2"	2 1/8"
1. Liquid piping	ft	111.45	83.01	27.56													
2. Gas piping	ft			111.45	42.49	40.49			27.56								
3. High pressure gas piping	ft																

Restriction of pipe length		Restriction (Based on installation manual)	Actual piping length	Equivalent piping length
1. Total piping length	ft	3281.00	233.79	
2. Maximum piping length	ft	656.00	90.26	90.75
3. Main pipe length	ft		27.56	
4. Piping length between the first branch and the farthest indoor unit	ft	148.00/295.01	62.70	
5. Level difference between outdoor and indoor unit(Max) (OD above ID unit / OD below ID unit)	ft	360.99/131.00	-9.84	
6. Level difference between indoor units	ft	164.04	3.28	

3) Basic and additional refrigerant amount

Basic refrigerant charge amount : 19.18 lbs

Additional refrigerant amount : 14.40 lbs

2.1.4 Piping

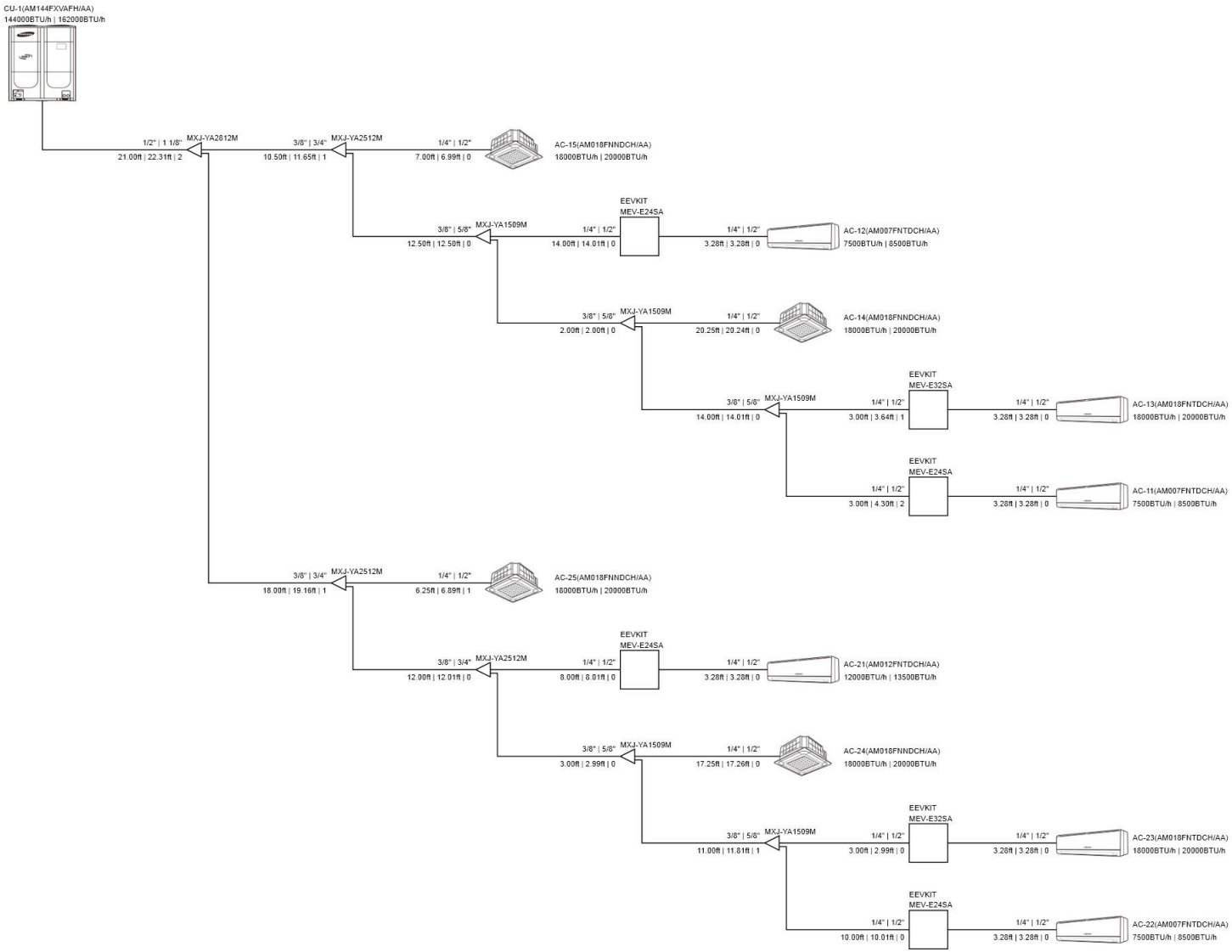

- The system configuration may be different from the actual installation conditions, refer to the installation manual.

2.1.5 Wiring

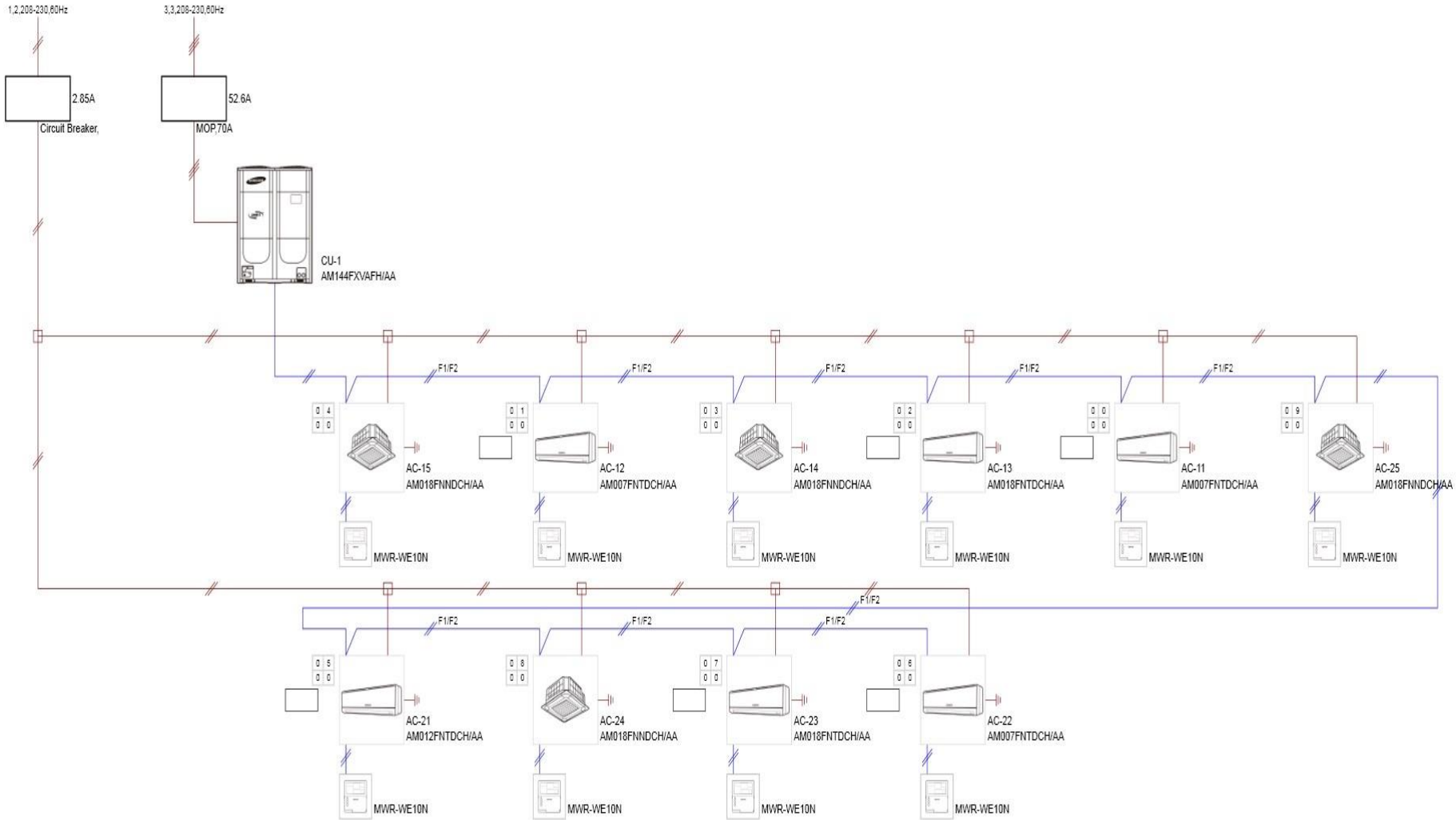

- The system configuration may be different from the actual installation conditions, refer to the installation manual.

3 Specification

3.1 DVM

3.1.1 Outdoor units

Model name				AM144FXVAFH/AA		
Power supply			Ø, #, V, Hz	3,3,208-230,60Hz		
Mode			-	HEAT PUMP		
Performance	HP/TON		HP/TON	15		
	Capacity(Nominal)	Cooling	kW	42.2		
			BTU/h	144000		
		Cooling 46°C	kW	-		
			BTU/h	N/A		
		Heating	kW	47.48		
			BTU/h	162000		
	-20 °C	Heating(Low ambient temp.)	kW	-		
			BTU/h	N/A		
Power	Power Input(Nominal)	Cooling	kW	11.86		
		Heating	kW	11.92		
	Power Input (at specific)		kW	N/A		
	Power Input(Nominal)	Cooling	A	33.7		
		Heating	A	33.8		
	Max. Current Input		A	52.6		
	Circuit Breaker		A	70		
COP	Cooling		-	3.56		
	Heating		-	3.98		
Compressor	Type		-	SSC Scrollx2		
	Output		kW × n	4.96x2		
Fan	Type		-	Propeller		
	Output		W	620x2		
	Number of Units		EA	2		
	Air Flow Rate		CFM	9535.32x2		
	External Static Pressure	Max.	W.G.	0.314959400619778		
Piping Connections	Liquid Pipe		Ø,mm(in)	12.7(1/2")		
	Gas Pipe		Ø,mm(in)	28.58(1 1/8")		
	Discharge Gas Pipe		Ø,mm(in)	-(-)		
	Oil Equalizing Pipe		Ø,mm(in)	N/A(N/A)		
Field Wiring	Power Source Wire		mm2	AWG		
	Transmission Cable		mm2	AWG/		
Refrigerant	Type		-	R410A		
	Factory Charging		lbs	19.18		
Sound	Sound pressure		dB(A)	62		
External Dimension	Net Weight		lbs	656.97		
	Shipping Weight		lbs	698.86		
	Net Dimensions (WxHxD)		in	50.98x66.73x30.11		
	Shipping Dimensions (WxHxD)		in	53.66x74.29x32.75		
Operating Temp. Range	Cooling		F	22.82~120.02		
	Heating		F	-4.18~75.02		

3.1.2 Indoor units

Model				AM007FNTDCH/AA	AM012FNTDCH/AA	AM018FNNDCH/AA	AM018FNTDCH/AA	
Power supply			Ø, #, V, Hz	1,2,208-230,60Hz	1,2,208-230,60Hz	1,2,208-230,60Hz	1,2,208-230,60Hz	
Performance	Capacity(Nominal)	Cooling	kW	2.198	3.5169	5.2753	5.2753	
			BTU/h	7500	12000	18000	18000	
		Cooling (SHC)	kW	1.4947	2.3446	3.9858	3.5755	
			BTU/h	5100	8000	13600	12200	
		Heating	kW	2.4911	3.9565	5.8614	5.8614	
			BTU/h	8500	13500	20000	20000	
Power	Power Input(Nominal)	Cooling	W	37	45	36	55	
		Heating		37	45	36	55	
	Current Input	Cooling	A	0.25	0.3	0.27	0.36	
		Heating		0.25	0.3	0.27	0.36	
Fan	Motor	Type	-	Crossflow Fan	Crossflow Fan	Turbo Fan	Crossflow Fan	
		Output	W	23	23	65	40	
		Number of unit	EA	1	1	1	1	
	Air Flow Rate	H/M/L (UL)	CFM	275.46/240.14/204.83	328.43/293.12/257.80	459.10/388.47/335.50	423.79/370.81/317.84	
	External Pressure	Min / Std / Max	W.G.	-	-	-	-	
Piping Connections	Liquid Pipe		Ø,mm(in)	6.35(1/4")	6.35(1/4")	6.35(1/4")	6.35(1/4")	
	Gas Pipe		Ø,mm(in)	12.7(1/2")	12.7(1/2")	12.7(1/2")	12.7(1/2")	
	Drain Pipe		Ø,mm	ID 18 HOSE	ID 18 HOSE	VP25 (OD 32,ID 25)	ID 18 HOSE	
Field Wiring	Power Source Wire		mm2	AWG 16~14	AWG 16~14	AWG 16~14	AWG 16~14	
	Transmission Cable		mm2	AWG 18/16	AWG 18/16	AWG 18/16	AWG 18/16	
Refrigerant	Type		-	R410A	R410A	R410A	R410A	
	Control Method		-	EEV NOT INCLUDED	EEV NOT INCLUDED	EEV INCLUDED	EEV NOT INCLUDED	
Sound	Sound pressure	High / Low	dBA	31/27	37/29	40/34	44/38	
Dimensions	Net Weight		lbs	18.73	18.73	26.45	27.55	
	Shipping Weight		lbs	24.25	24.25	30.86	34.17	
	Net Dimensions (WxHxD)		in	32.48x11.22x7.44	32.48x11.22x7.44	22.63x9.84x22.63	41.92x11.73x8.58	
	Shipping Dimensions (WxHxD)		in	35.59x13.89x10.35	35.59x13.89x10.35	24.52x11.73x25.70	44.80x14.88x11.85	
Panel Size	Panel model		-			PC4SUSMEN		
	Panel Net Weight		lbs			5.95		
	Shipping Weight		lbs			9.25		
	Net Dimensions (WxHxD)		in			26.37x1.77x26.37		
	Shipping Dimensions (WxHxD)		in			28.11x4.17x28.50		

4 Controller

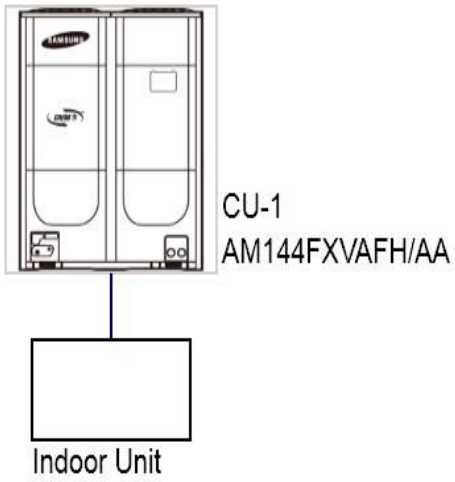

- The system configuration may be different from the actual installation conditions, refer to the installation manual.

5 Total Equipment List

Index	Model	Qty	Remark(Categories)	Unit Price	Amount
Outdoor unit	AM144FXVAFH/AA	1	DVM S(NEW)	0	0
Indoor unit	AM018FNNDCH/AA	4	4 WAY CASSETTE (600x600)	0	0
	AM007FNTDCH/AA	3	NEO FORTE	0	0
	AM012FNTDCH/AA	1	NEO FORTE	0	0
	AM018FNTDCH/AA	2	NEO FORTE	0	0
Piping	MEV-E24SA	4	Distributor Kit	0	0
	MEV-E32SA	2	Distributor Kit	0	0
	MXJ-YA2812M	1	Y-Joint	0	0
	MXJ-YA2512M	3	Y-Joint	0	0
	MXJ-YA1509M	5	Y-Joint	0	0
Control System	MCM-A202DN	1	ON/OFF Controller	0	0
	MIM-B17N	1	BACnet Gateway	0	0
Optional accessories	MWR-WE10N	10	WIRED REMOTE CONTROLLER	0	0
	PC4SUSMEN	4	4 WAY CASSETTE (600x600) PANEL	0	0
Ref. Pipe	6.35(1/4")	111.45	ft	0	0
	9.52(3/8")	83.01	ft	0	0
	12.70(1/2")	139.01	ft	0	0
	15.88(5/8")	42.49	ft	0	0
	19.05(3/4")	40.49	ft	0	0
	28.58(1 1/8")	27.56	ft	0	0
Additional Ref. Quantity	R410A	14.4	lbs	0	0
		Total			**0**